Unclassified
SECURITY CLASSIFICATION OF THIS PAGE

DTIC FILE COPY

REPORT DOCUMENTATION PAGE

AD-A197 752

1b. RESTRICTIVE MARKINGS

3. DISTRIBUTION/AVAILABILITY OF REPORT
Approved for public release;
Distribution unlimited.

2b. DECLASSIFICATION/DOWNGRADING SCHEDULE

4. PERFORMING ORGANIZATION REPORT NUMBER(S)

5. MONITORING ORGANIZATION REPORT NUMBER(S)
AFOSR-TR- 88-0728

6a. NAME OF PERFORMING ORGANIZATION: University of Illinois at Chicago

6b. OFFICE SYMBOL (If applicable)

7a. NAME OF MONITORING ORGANIZATION: Air Force Office of Scientific Research

6c. ADDRESS (City, State and ZIP Code): P.O. Box 4348 M/C 273, Chicago, IL 60680

7b. ADDRESS (City, State and ZIP Code): Electronic and Material Sciences, Bolling Air Force Base, DC 20332-6448

8a. NAME OF FUNDING/SPONSORING ORGANIZATION: Air Force Office of Scientific Research

8b. OFFICE SYMBOL (If applicable)

9. PROCUREMENT INSTRUMENT IDENTIFICATION NUMBER: #F49620-87-C-0021

8c. ADDRESS (City, State and ZIP Code): Electronic and Material Sciences, Bolling Air Force Base, DC 20332-6448

10. SOURCE OF FUNDING NOS.

PROGRAM ELEMENT NO.	PROJECT NO.	TASK NO.	WORK UNIT NO.
61102F	DARPA		

11. TITLE (Include Security Classification): Unclassified ("MBE Growth, Characterization...

12. PERSONAL AUTHOR(S): Dr. Jean-Pierre Faurie

13a. TYPE OF REPORT	13b. TIME COVERED	14. DATE OF REPORT (Yr., Mo., Day)	15. PAGE COUNT
Semi Annual	FROM 11/13/86 TO 11/12/89	December 31, 1987	20

16. SUPPLEMENTARY NOTATION

DTIC ELECTE AUG 16 1988 S E D

17. COSATI CODES		
FIELD	GROUP	SUB GR.

18. SUBJECT TERMS (Continue on reverse if necessary and identify by block number)

19. ABSTRACT (Continue on reverse if necessary and identify by block number)

Here we report on growth and characterization of high quality HgCdTe epilayers, MBE growth and characterization of two-inch diameter p- and n-type $Hg_{1-x}Cd_xTe$ films on GaAs(100) substrate. ~~We discuss~~, the n-type intrinsic and extrinsic doping. The incorporation of As has been photo assisted using a Nd-YAG pulsed laser.

X-ray photoemission of Hg clusters on $Hg_{1-x}Cd_xTe$ surfaces has been studied.

Direct measurement by XPS and electrical determination of HgTe-CdTe valence band discontinuity give values of 300-400 meV at 300K.

Silicon has been used as a n-type dopant to grow a homojunction which electrical characteristics are presented here.

20. DISTRIBUTION/AVAILABILITY OF ABSTRACT
UNCLASSIFIED/UNLIMITED ☒ SAME AS RPT. ☐ DTIC USERS ☐

21. ABSTRACT SECURITY CLASSIFICATION: Unclassified

22a. NAME OF RESPONSIBLE INDIVIDUAL	22b. TELEPHONE NUMBER (Include Area Code)	22c. OFFICE SYMBOL
Captain Kevin Malloy	(202) 767-4931	NE

DD FORM 1473, 83 APR — EDITION OF 1 JAN 73 IS OBSOLETE.

Unclassified
SECURITY CLASSIFICATION OF THIS PAGE

MBE GROWTH, CHARACTERIZATION AND ELECTRONIC DEVICE PROCESSING OF HgCdTe, HgZnTe, RELATED HETEROJUNCTIONS AND HgCdTe-CdTe SUPERLATTICES

DARPA - AFOSR - F49620-87-C-0021
November 13, 1986 - November 12, 1989

Semi Annual Technical
December 31, 1987

Jean-Pierre Faurie
University of Illinois at Chicago

I. Growth and Characterization of high quality HgCdTe epilayers

A strong emphasis has been laid recently on the characterization of HgCdTe epilayers by double X-ray rocking curve. A careful examination of what has been up to now reported is far from being conclusive.

In fact what is claimed as world record is only one particular point on a crystal. Above all, nobody has presently established a clear relationship between the FWHM of X-ray Rocking Curve peak and the electrical characteristics of this HgCdTe layer.

We have just received our X-ray equipment during the Summer 87 and have started our own investigations. What we have in mind is (1) to understand the relationship between FWHM of the substrate - FWHM of the epilayer, (2) to establish a relationship between FWHM mobility and carrier lifetime for a given HgCdTe MBE layer grown under very well established growth conditions.

We have already characterized numerous substrates and HgCdTe epilayers grown in the (111) orientation on CdTe and CdZnTe substrates. Our preliminary conclusions are the following:

1 - if we want to do marketing with a FWHM of 17 arc see (Fig. 1) for a HgCdTe layer we can claim to have presently the world record.

2 - if we want to do material science we have to conclude that these values are not representative of what is currently obtained. In addition to that FWHM values are highly non uniform over the same epilayer. This problem, in our case, is without any doubt due to the non uniformity of CdTe and CdZnTe substrates (Fig. 1 to 7).

When the substrate is uniform enough, we have found that the FWHM of the epilayer is about 1.5 times larger than the half width of the substrate if it is CdZnTe and about 2 times if the substrate is CdTe (Fig. 8 to 10).

3 - Due to this lack of uniformity in the substrate quality it is not surprising that no correlation has been yet established between epilayer physical properties and FWHM. We are currently working on this problem.

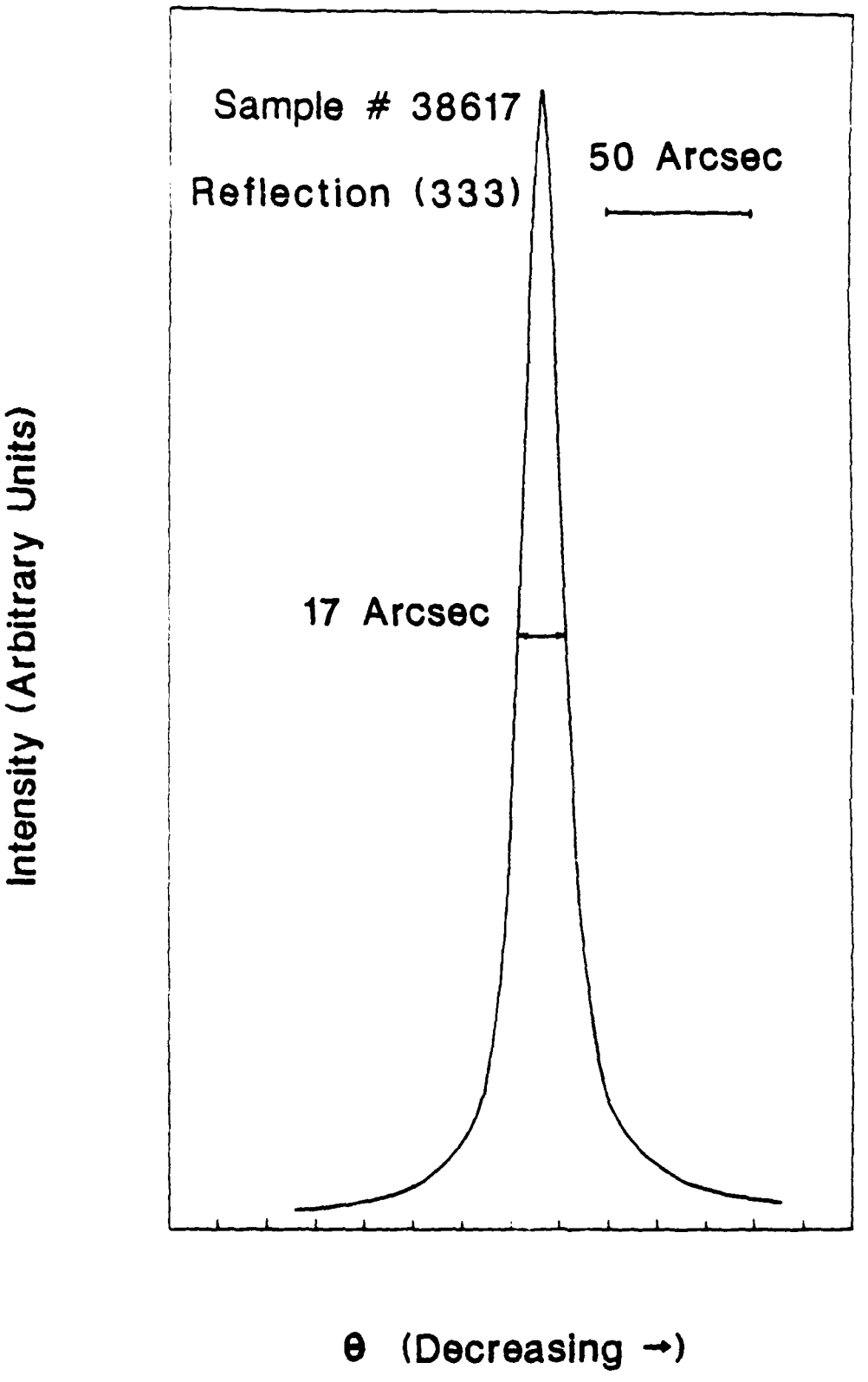
Sample # 38617
Reflection (333)
50 Arcsec
17 Arcsec
Intensity (Arbitrary Units)
θ (Decreasing →)

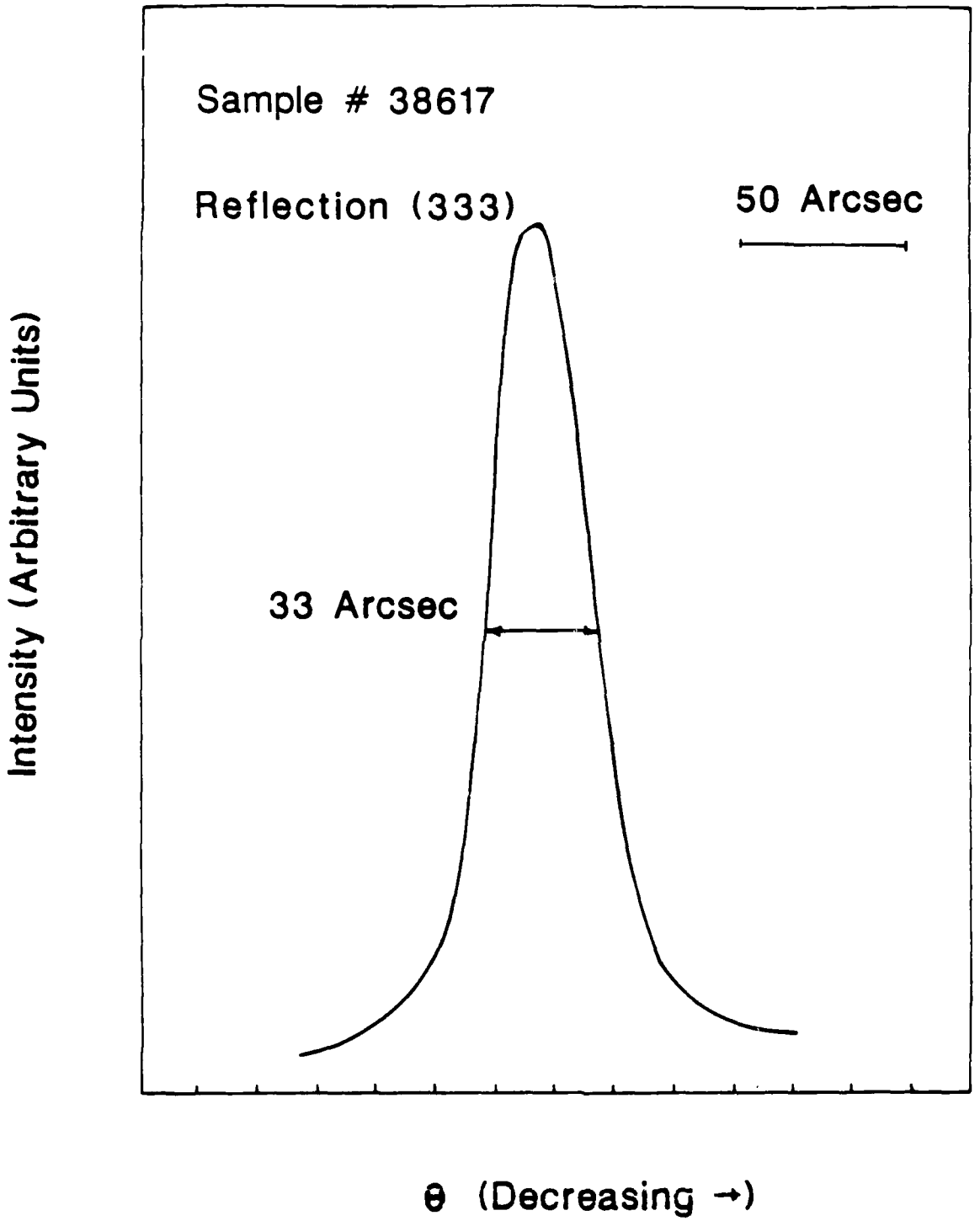
Sample # 38617
Reflection (333)
50 Arcsec
33 Arcsec
Intensity (Arbitrary Units)
θ (Decreasing →)

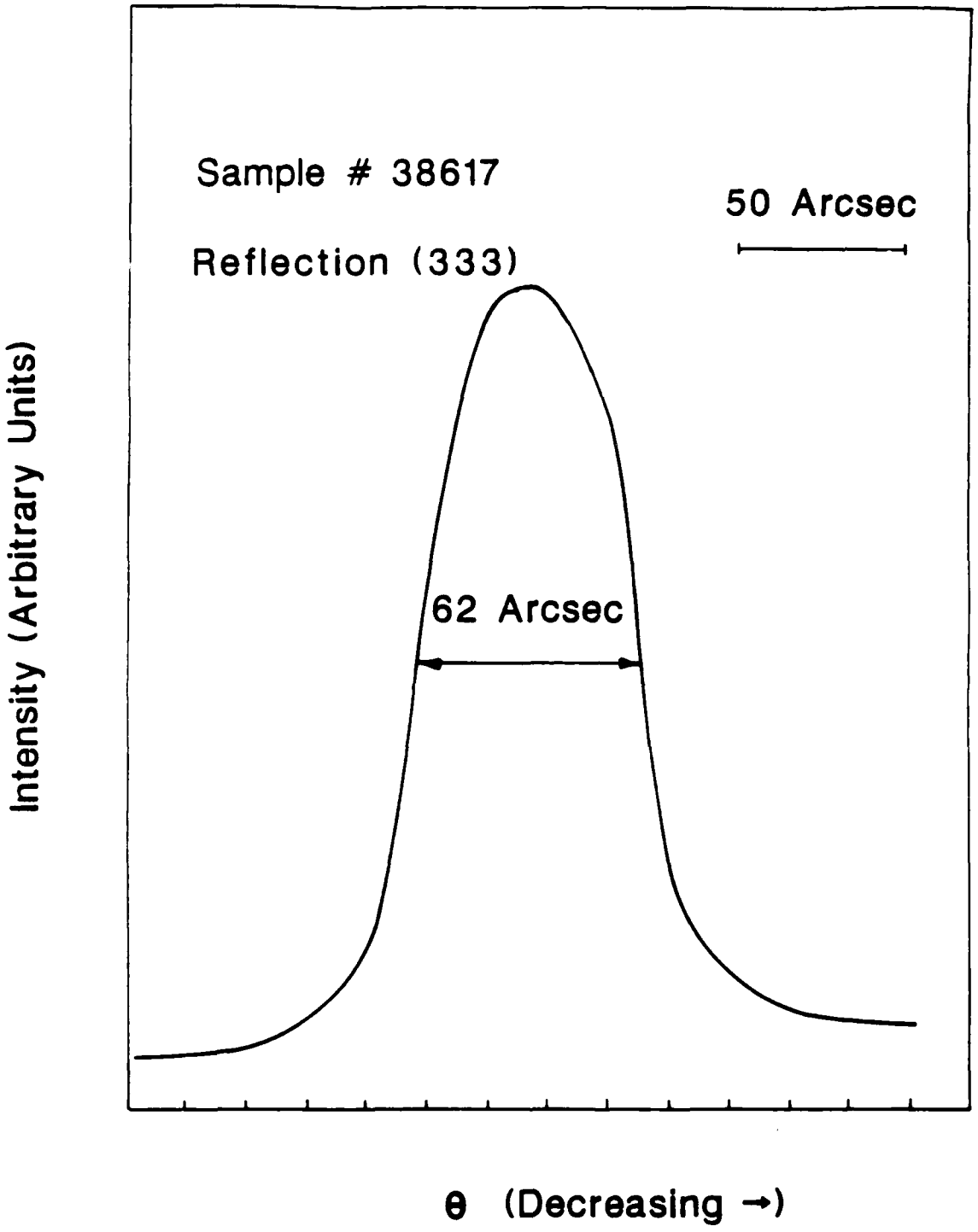
Sample # 38617
Reflection (333)
50 Arcsec
62 Arcsec
Intensity (Arbitrary Units)
θ (Decreasing →)

Sample # 38617

Substrate: CdZnTe

Layer Thickness: 5 μm

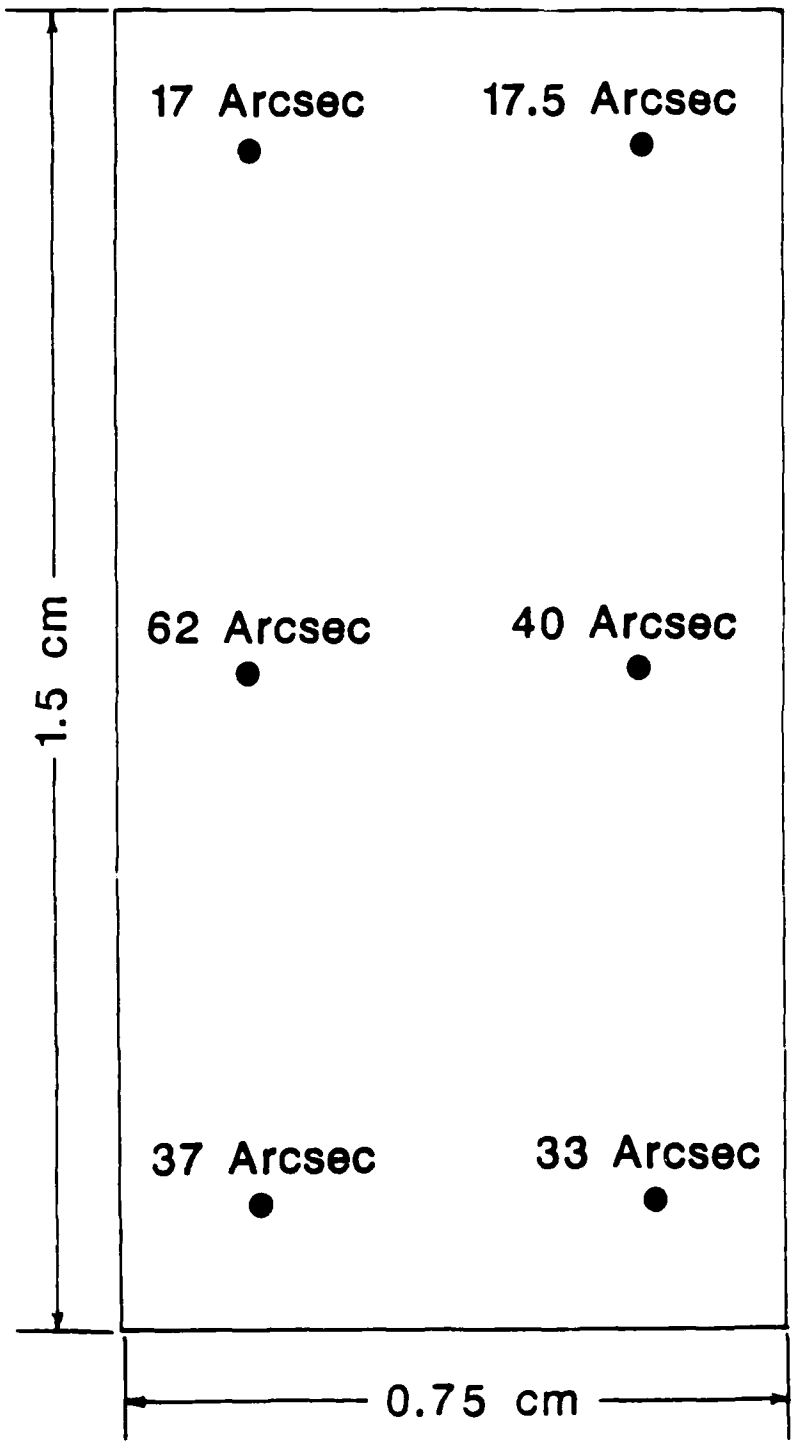

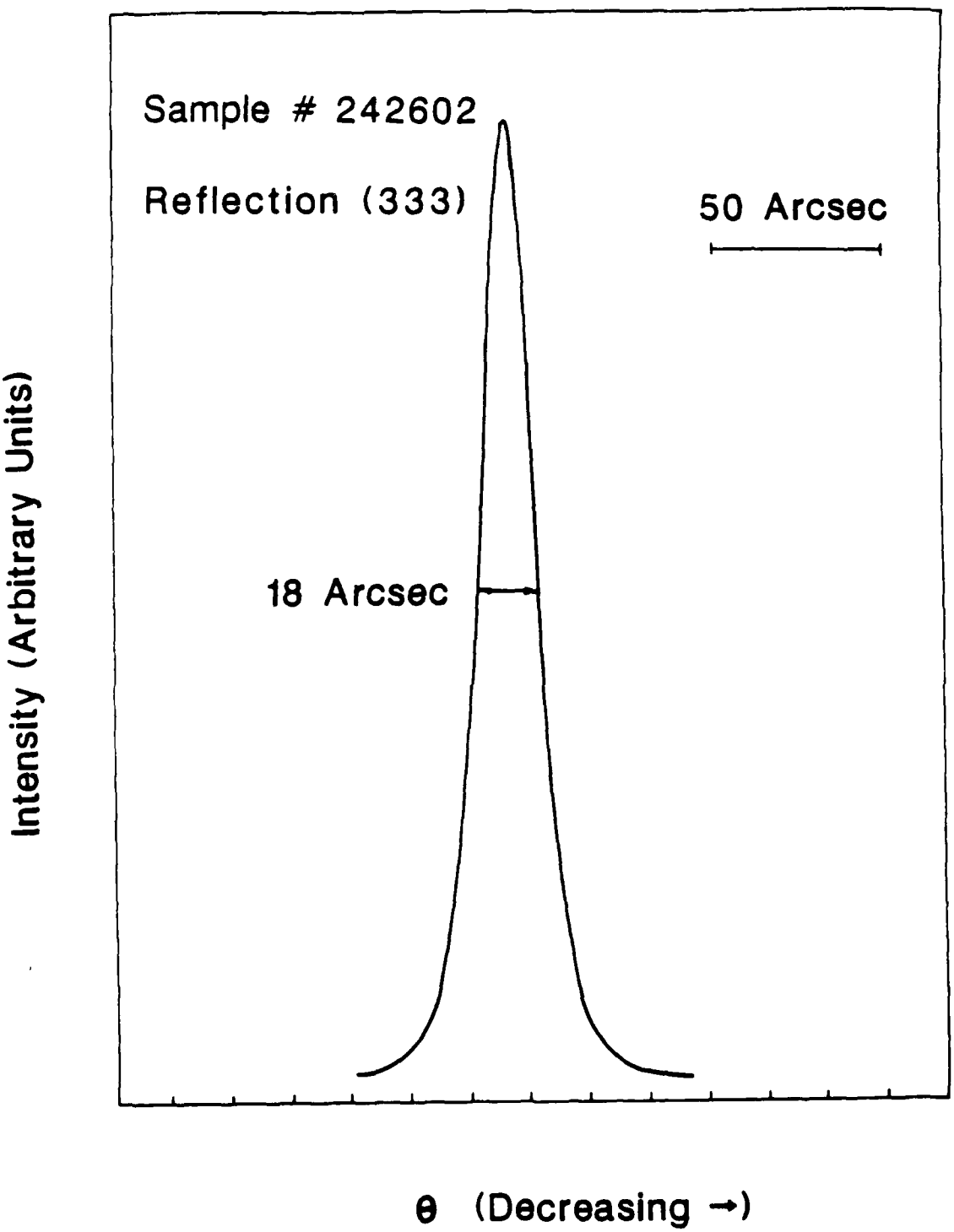
Sample # 242602
Reflection (333)
50 Arcsec
18 Arcsec
Intensity (Arbitrary Units)
θ (Decreasing →)

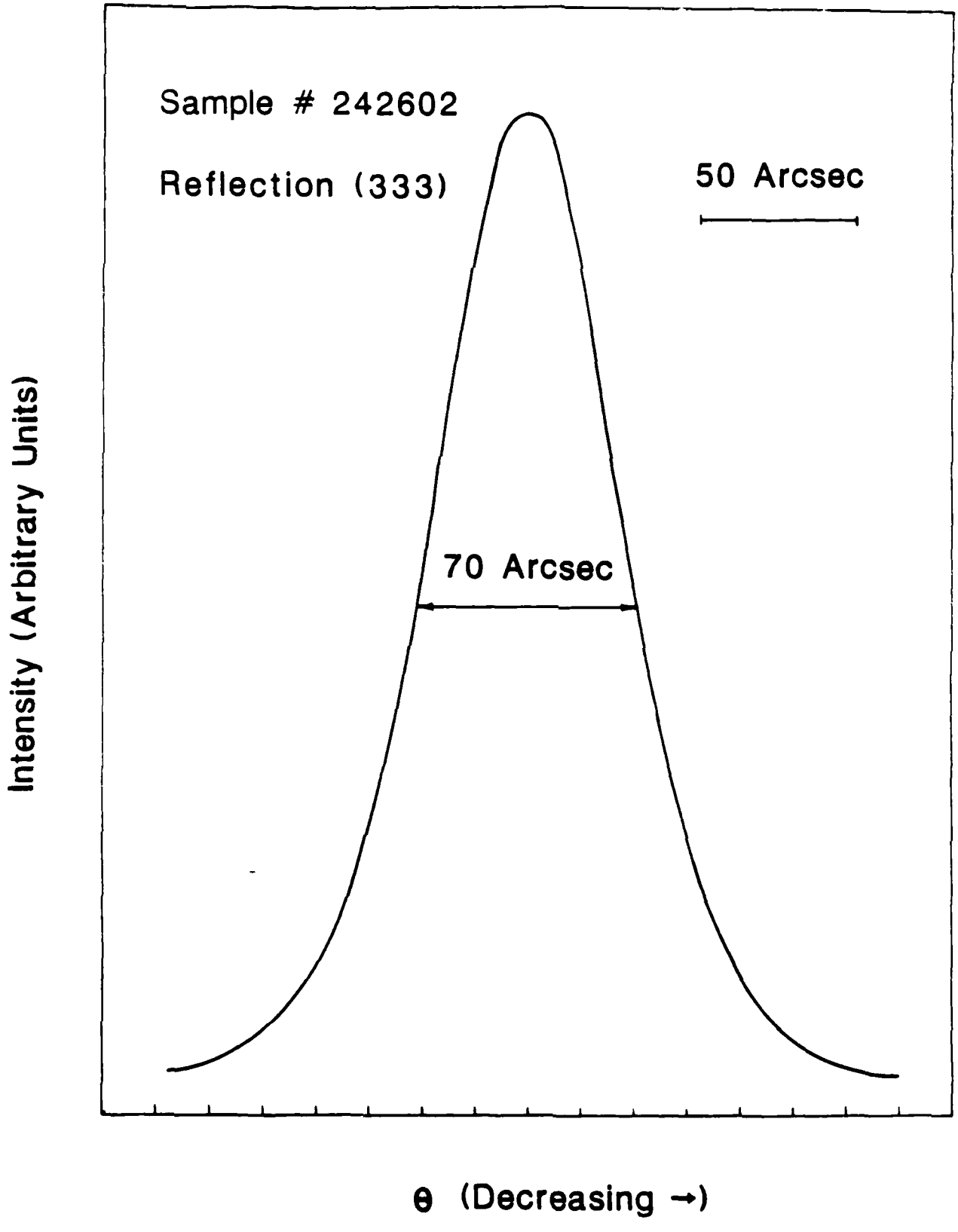
Sample # 242602
Reflection (333)
50 Arcsec
70 Arcsec
Intensity (Arbitrary Units)
θ (Decreasing →)

Sample # 242602

Substrate: CdTe

Layer Thickness: 12.1 μm

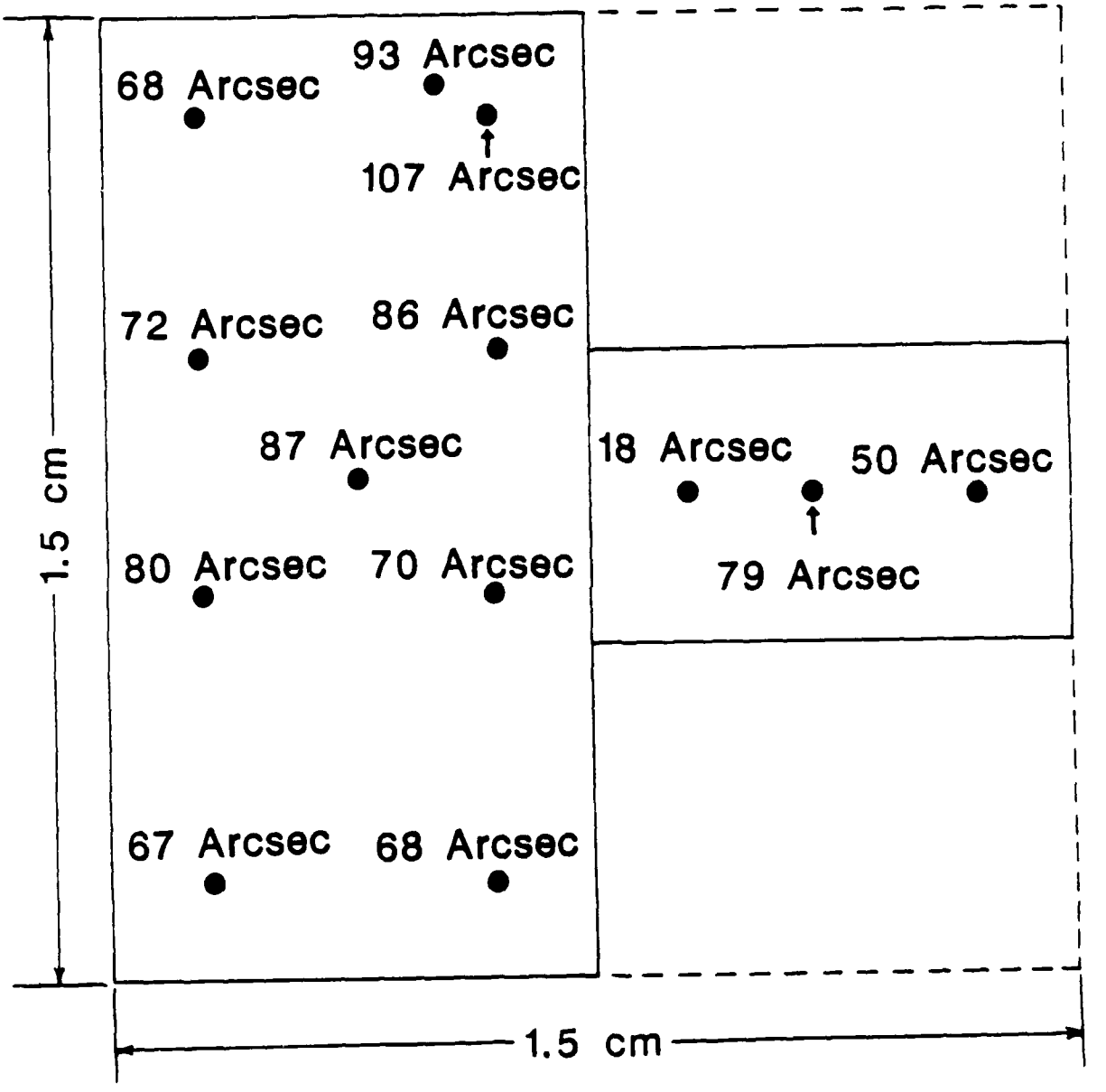

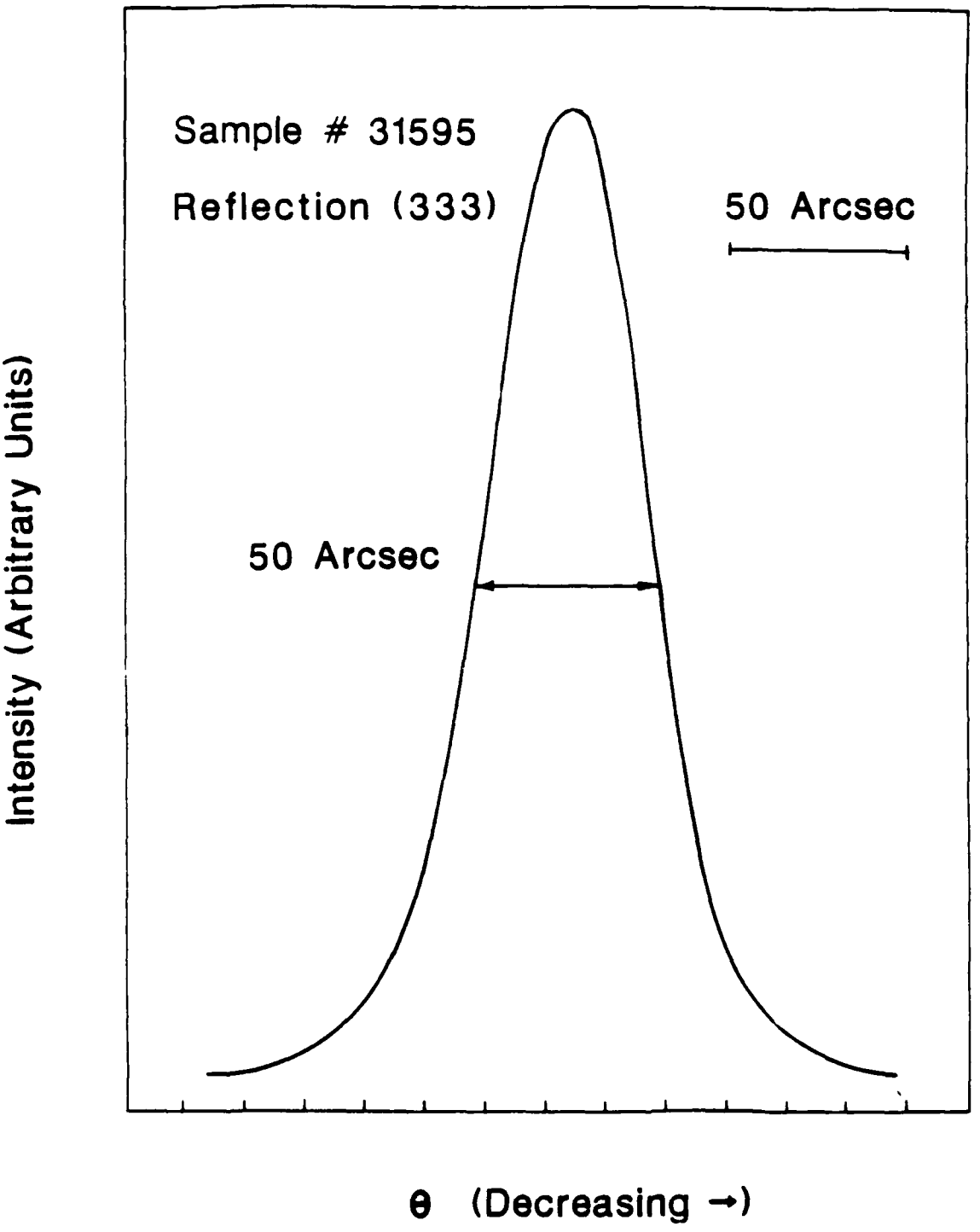
Sample # 31595
Reflection (333)
50 Arcsec
50 Arcsec
Intensity (Arbitrary Units)
θ (Decreasing →)

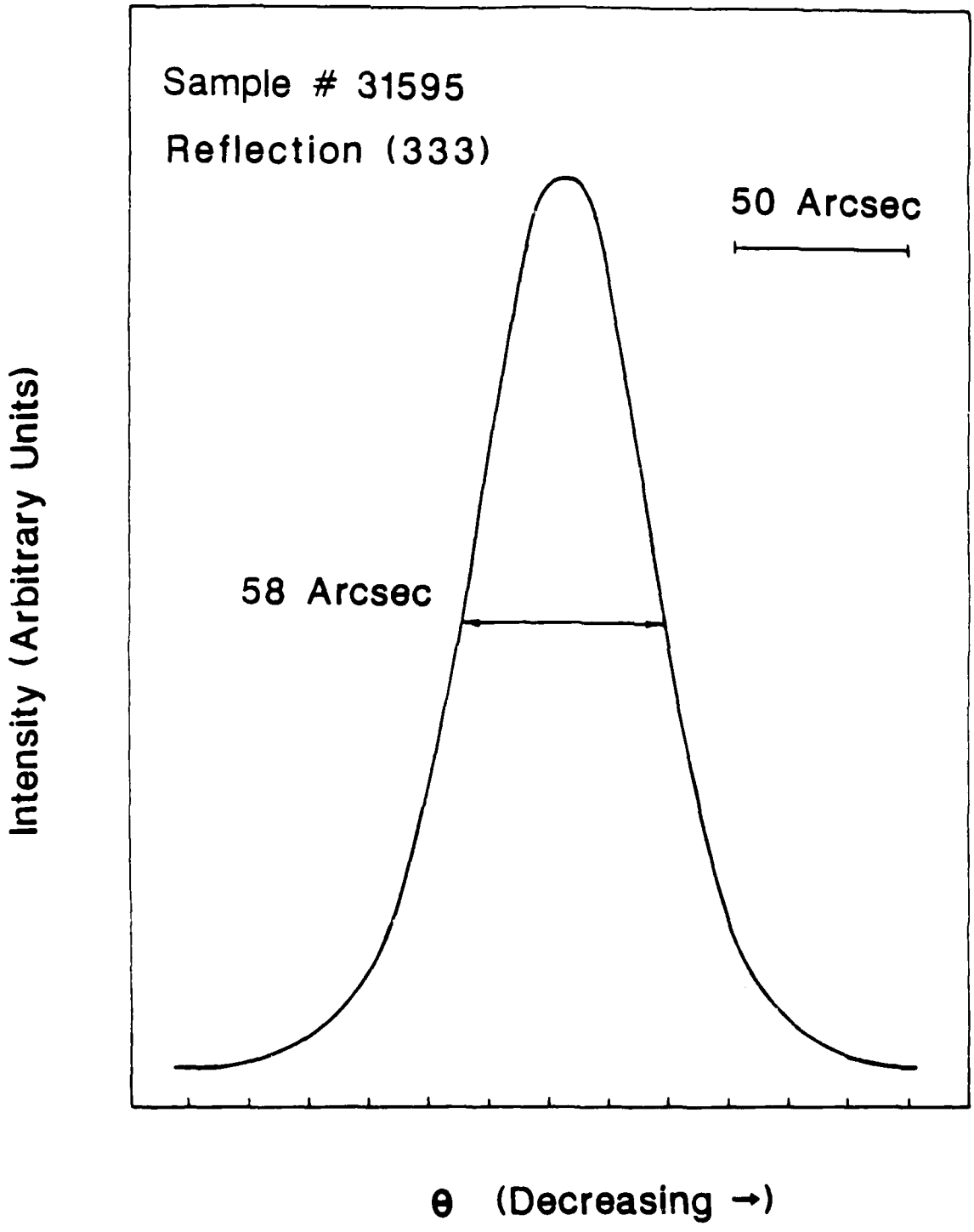
Sample # 31595
Reflection (333)
50 Arcsec
58 Arcsec
Intensity (Arbitrary Units)
θ (Decreasing →)

Sample # 31595

Substrate: CdZnTe (37 Arcsec)

Layer Thickness: 9.6 μm

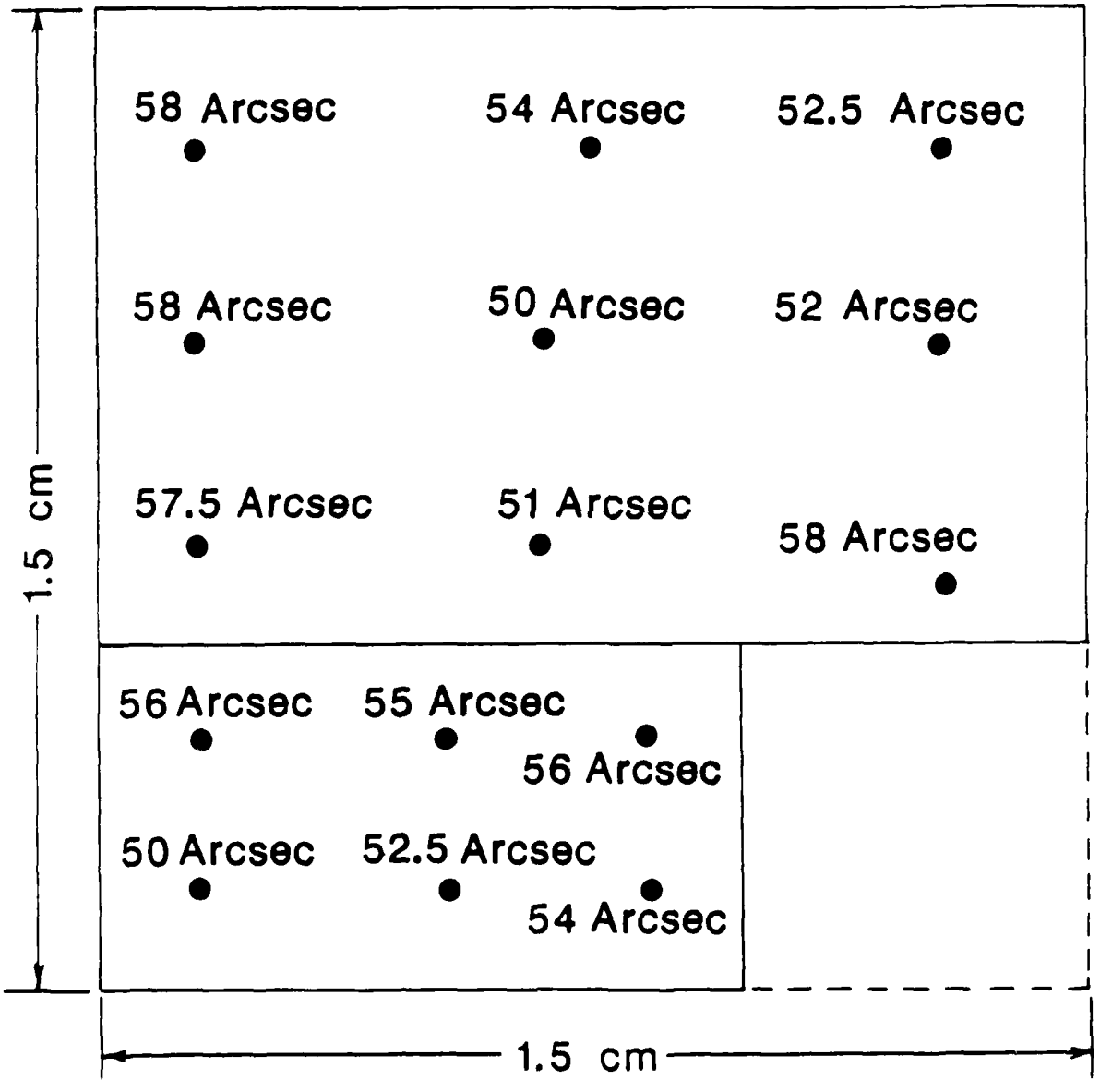

II. MBE growth and characterization of two-inch diameter p-and n-type $Hg_{1-x}Cd_xTe$ films on GaAs(100) substrate.

The growth of a p-type layers on a two-inch GaAs(100) substrate has been previously reported (June 15, 1987 report). Since then we have grown several p- and n-type HgCdTe layers on 2 inch GaAs substrates.

Their surfaces were shiny and mirror-like from center to edge. Their thicknesses were uniform within 0.6%. Their Cd concentrations (x) were very uniform, exhibiting standard deviations $\Delta x/x$ as low as 0.7%. These films were completely uniform in their conduction types, that is, the n-type films were entirely n-type, and likewise for the p-type films. The Hall mobilities of these films show them to be of high quality, with values as high as 6.7×10^2 $cm^2V^{-1}s^{-1}$ for p-type ($x=0.22$), and 1.8×10^5 $cm^2V^{-1}s^{-1}$ for the n-type films ($x=0.21$). These results represent an important achievement towards the future of infrared detector technology.

For more detail see the attached paper published in Applied Physics Letters entitled "Molecular Beam Epitaxial Growth and Characterization of Two-Inch Deameter $Hg_{1-x}Cd_xTe$ Films on GaAs(100) Substrates."

III. Recent achievements in the growth by MBE of $Hg_{1-x}Cd_xTe$

In the attached paper to be published in the Journal of Vacuum Science and Technology experimental data on the influence of the substrate temperature on the Cd composition and on the growth rate when this temperature is above T_{max} (see the quarterly report of June 15, 1987 for the definition of T_{min} and T_{max}) are presented.

In this paper updated data on the best electrical performances of p-type and n-type HgCdTe epilayers grown by MBE are also included.

This paper is entitled "New Achievements on $Hg_{1-x}Cd_xTe$ Grown by Molecular Beam Epitaxy."

III. N-type layers by stoichiometric adjustment

Although p-type layers are usually grown by MBE in the (111)B orientation

(Quarterly Report March 15, 1987). High mobility N-type layers can also be achieved by MBE. As it was mentioned before, differences exist between the (111)B and the (100) orientation in terms of maximum doping level. If $2\times10^{16}cm^{-3}$ is never exceeded for (111) n-type fiims even under an extremely high Hg flux, which produces twins, doping level in the 5×10^{16}-1×10^{17} cm^{-3} range has been obtained for (100) films.

Another important difference is observed in the shape of the Hall carrier concentration vs reciprocal temperature curve. Whereas the curves for (100) epilayers can be very well fitted using the model of a fully ionized impurity it is not the case for most of the (111)B epilayers. For (111)B epilayers in the intrinsic region, the value of the carrier concentration decreases more slowly with temperature and in the extrinsic part the carrier concentration level is not completely flat. This gives a large rounded shape zone between the two regimes.

These two differences seem to indicate that the origin of the doping is different in the two orientations. In the (100) orientation the curve is identical to Hall carrier concentration curve of intentionally doped HgCdTe using In or Si. Therefore, one can conclude that the n-type character in this orientation is linked to an electrically active impurity. Concerning the (111)B orientation a single impurity level is not consistent with the Hall curve behavior. Impurity bands occurring inside the bandgap might provide a better agreement. Another hypothesis is also proposed. In the (111)B orientation most of the layers are p-type but when E_g is small, i.e. when $x \leq 0.20$, the number of electron is high, μ_e/μ_{HH} is also high and E_g decreases with temperature. This could prevent the transport properties from being dominated by the acceptors at low temperature, but also would give a mixed behavior.

Some (111)B layer exhibit a "normal" n-type character. In that case it seems legitimate to conclude that it is due to an active impurity.

Now an important question has to be raised. What is the impurity active in (100) which is not in (111)B. In fact, numerous SIMS investigations have shown that impurity levels are low in MBE layer and also that these levels are the same in the two orientations. Therefore, the answer is probably not related to a foreign impurity. An explanation has been recently proposed (1). This active impurity would be the tellurium itself. It has be seen later that with the exception of the Group I elements all the impurities tested so far are incorporated as donors.

Since MBE layers are most of the time grown under Te rich conditions the

tellurium in excess is first incorporated in the material up to the limit of solubility at the substrate temperature. Beyond this limit, depending of the substrate temperature it can be completely reevaporated if Ts is above 195°C or it will crystallize preventing the HgCdTe film to be monocrystalline.

The Te precipitates whether they are formed and incorporated during the growth or they are produced during the cooling process are not supposed to be electrically active.

It is still unclear why the tellurium can be incorporated as an electrically active dopant in (100) orientation and not in (111)B. It is certainly related to the bounding. In the (100) orientation the Te atoms are certainly incorporated in Hg vacancies and are part of the lattice, whereas in the (111)B orientation they are not, and would produce a twinning before the polycrystalline growth.

This explanation about the tellurium being involved as an active dopant in the (100) orientation presents also the interest of explaining why layers are n-type in the (100) orientation despite the fact that the Hg sticking coefficient is less in this orientation than in the (111)B. As discussed before, this was a puzzling problem because the (100) layers should have more Hg vacancies than (111)B layers and therefore should be more p-type.

REFERENCES:

J.P. Faurie - HgCdTe MBE workshop. Washington (Nov. 1987)

I. As doping: Photo assisted MBE growth

In a previous report (March 15, 1987) it has been shown that under regular MBE growth conditions As and Sb are incorporated as donors in HgCdTe. Exposure to a U.V. Xenon Lamp of 1kW increased the N_D-N_A level when As was used.

In the previous report it was not concluded that As or Sb cannot be incorporated as p-type dopants in MBE grown layers. But it was clear that it is not a problem to solve. In order to find out the proper conditions to incorporate, if possible, the As in the p-type site a Nd-YAG pulsed laser operating at 0.523μm was used during the growth process.

Numerous experiments were carried out. For the sake of clarity only some of them are reported in Table I.

TABLE I

Photo assisted MBE growth
Nd: YAG LASER - Green light
Growth Temperature

Sample	x	t(μm)	Growth rate layer HgTe	CdTe		cc(cm^{-3})	Laser power mw/cm_2	T_{As}
CZT48HCT659	.245	2.57	7.14	5.39	1.75	n-9.10x10^{15}	160	150
CZT49HCT660	.240	2.58	7.17	5.45	1.72	n-2.80x10^{15}	0	150
CZT50HCT661	.300	2.18	6.06	4.25	1.81	n-1.12x10^{16}	500	175
CZT52HCT663	.230	---	---	---	---	n-3.50x10^{15}	0	175
CZT51HCT662	.280	2.25	6.25	4.50	1.75	n-2.65x10^{15}	500	150
CT277HCT685	.260	2.94	6.53	4.84	1.69	n-1.22x10^{15}	0	125
CZT69HCT686	.270	3.02	6.71	4.90	1.81	n-1.45x10^{15}	25	125
CT278HCT687	.265	3.02	6.71	4.92	1.79	n-7.24x10^{15}	50	125

From Table I it is clear that with or without the laser light during MBE growth As behave as a donor in HgCdTe layers. With the laser it has been observed a decrease of the Hg sticking coefficient. At low power the Hg vacancy density increases, which enhances the p-type character. At high power, not only the stoichiometry but also the composition x changes. In the presence of arsenic during growth the n-type character observed without light in the (111)B orientation is in fact enhanced because more Hg vacancies are available for As atoms.

These experiments confirm those reported in March 1987. However, they cannot completely rule out the possibility of incorporating As in the right site. A lower growth temperature, a higher Hg flux, a different crystallographic orientation or a different laser (cw for example) have to be investigated before making any definite conclusion.

It is important to add that a very important cross contamination due to residual

arsenic has been observed.

V. X-ray photoemission study of Hg clusters on $Hg_{1-x}Cd_xTe$ surfaces

The (111)B surface of MBE-grown $Hg_{1-x}Cd_xTe$ samples has been studied in detail using x-ray photoemission spectroscopy (XPS). The composition of the samples was in the range x = 0.15 to 0.97. The smaller x values were obtained with three MBE sources (CdTe, Te and Hg) as usual, whereas only two sources (CdTe and Hg) were used to obtain the larger values. A monochromatized and focussed Al K_α excitation line was used for the XPS measurements.

Two types of Hg have consistently been found for all the samples. These two types of Hg will be labeled $Hg^{(1)}$ and $Hg^{(2)}$ hereafter. From the binding energy with respect to the valence-band maximum, $Hg^{(1)}$ is clearly identified as Hg in HgCdTe. The second component is found at higher binding energy and is attributed to the presence of small Hg clusters on the HgCdTe surface. The radius of these clusters is deduced from the $Hg^{(2)}4f_{7/2}$ intensity measured with XPS. Values between 15Å and 40Å are obtained. The $Hg^{(2)}4f_{7/2}$ binding energy increases with decreasing cluster size. This is explained by the Coulomb energy ~ e^2/r due to the unit charge appearing on the cluster during the photoemission process[1]. This charge is not neutralized within the time scale relevant for photoemission, due to the semiconducting nature of the substrate. A good agreement between the experimentally observed binding energy shift and the calculated e^2/r behavior is observed. For large cluster sizes, a binding energy of 100.2 ± 0.2 eV is deduced. This is close to the value for bulk Hg (99.9 eV)[2].

The apparent spin-orbit splitting of the $Hg^{(2)}5d$ levels decreases with decreasing cluster size. A total variation of 0.5 eV is measured. Our results are smaller than the value for free Hg atoms, except for the largest cluster sizes. This is attributed to the repulsion between the Cd4d and Hg5d levels, as initially discussed by Moruzzi et al.[3]

From the influence of the sample preparation conditions on the amount of Hg in the clusters, we conclude that Hg outdiffusion is probably the major reason for the formation of these clusters.

Ref.: (1) G.K. Wertheim et al., Phys. Rev. Lett. 51, 2310 (1983), (2) S. Svensson et al., J. Elec. Spectros. 9,51 (1976), (3) V. L. Moruzzi et al., Phys. Rev. B10, 4856(1974).

For more detail see the attached paper accepted for publication in Physical Review, entitled "X-ray Photoemission from Small Mercury Clusters on II-VI

Semiconductor Surfaces."

VI. Valence band discontinuity at the HgTe-CdTe

The valence band discontinuity (ΔE_V) of the HgTe-CdTe heterojunction has recently attracted much attention. However, our knowledge of this value is far from being complete. There is much controversy, both theoretical and experimental, concerning its value. The magneto-optical and resonant Raman scattering[1] measurements performed at low temperature yield a value of less than 120meV for ΔE_V of the HgTe-CdTe(111)B heterojunction. This result agrees with the prediction of the common anion rule[2]. The core level X-ray photoelectron spectroscopy (XPS) measured 0.36eV[3,4] at room temperature in agreement with other theoretical predictions[5,6]. The method of determination using only the cation core level difference is questionable because there is no proof that the difference between the core level and the valence band maximum in the two semiconductors does not change when the heterojunction is formed. This change, which could be due to band bending and/or interface chemical effect, would make such an indirect determination inappropriate. Therefore, we have investigated the valence band structure (VBS) of the heterojunction and present here the first direct measurement of the valence band discontinuity of the HgTe-CdTe heterojunction.

The HgTe-CdTe(111)B interface was grown in the MBE chamber and transferred under UHV conditions into the analysis chamber. The thickness of the thin overlayer, as determined from the core level XPS peak area, was chosen between 15Å and 30Å. The X-ray source used here is the Al $K_{\alpha_{12}}$ line which has the energy of 1486.6eV.

Since the escape depth of the valence electrons of the interface, here, is comparable with the thickness of the overlayer, the interface XPS spectrum covers the VBSs of the overlayer, substrate, and interface region. We have reported that the intensities of the substrate and overlayer core level peaks vary with thickness in a manner consistent with an exponential attenuation, indicating that the interface is abrupt in the monolayer range[1]. In other words, the interface region is so narrow that the contribution of it in the interface XPS spectrum of the VBS can be neglected.

The principle of the direct measurement of the ΔE_V of HgTe-CdTe interface is to deconvolute the VBS of the interface spectrum using the normalized HgTe and CdTe valence band distribution. This normalization considers two parameters.

One is the attenuated intensities of the clean substrate due to the overlayer. The other one is energy shifts due to the interface band-bending effect. After least-square fitting process, the value of ΔE_V can be obtained. We report here that the best fit gives an average value of 0.40eV for the valence band discontinuity of HgTe-CdTe(111)B interface with different thicknesses and growth sequences. This result agrees with the result measured from the core level XPS method[3,4]. We have also extended this method to the measurement on the ΔE_V of the HgTe-CdTe heterojunction in the (100) orientation and found that ΔE_V is equal to 0.290 eV.

1. J.P. Faurie, C. Hsu, and Tran Minh Duc, J. Vac. Sci. Technol. A5, 3074 (1987) and references therein.
2. J. O. McCaldin, T. C. McGill and C. A. Mead, Phys. Rev. Lett. 36, 56 (1976).
3. S. P. Kowalczyk, J. T. Cheung, E. A. Kraut, and R. W. Grant, Phys. Rev. Lett. 56, 1605 (1986).
4. Tran Minh Duc, C. Hsu, and J.P. Faurie, Phys. Rev. Lett. 58, 1127 (1987).
5. J. Tersoff, Phys. Rev. Lett. 56, 2755 (1986).
6. S. H. Wei and A. Zunger, Phys. Rev. Lett. 59, 144 (1987).

B-Electrical determination

Several $Hg_{1-x}Cd_xTe$-CdTe-$Hg_{1-x}Cd_xTe$ heterostructures with different x, doping level and barrier thickness have been grown by MBE at the University of Illinois.

The study of the current voltage behavior resulted in a determination of a valence-band discontinuity ΔE_V = 390 ± 75meV at T = 300K. This result is in reasonable agreement with XPS results.

This work has been done in collaboration with Prof. McGill group at Caltech.

For more details see the attached paper published in Applied Physics Letters (Dec. 1987)

VII. Si-doped $Hg_{1-x}Cd_xTe$ homojunctions grown in situ by MBE

The first homojunctions with x = .27 were also measured recently. The bottom layer with a thickness of 4.2μm was doped to $2\times10^{16}cm^{-3}$ p-type by stoichiometry deviation, whereas the top layer with a thickness of 1μm was doped to $4\times10^{16}cm^{-3}$ n-type by silicon incorporation during the growth. A strong rectification is seen (fig. 5) when the top material is biased negatively as expected. The quality factor varies from 2.2 at 110K to 3.0 at 80K. The R_0A shows a two sloped variation

versus 1/T as commonly seen in this case (fig. 12). The values reached at 80K vary from 15 to 40 Ωcm^2 from device to device. Even though the photoresponse has not been measured yet, we saw that the devices are sensitive to the infrared, the photocurrent generated having the proper polarity at zero bias (reverse current). The capacitance measured at zero volt is consistent with the expected doping levels, the depletion width being shared between the two sides of the function. It decreases with reverse bias, but $1/C^2$ does not follow a straight line versus voltage (fig. 13) indicating that the doping level is not uniform. We think that even though the junction was intentionally grown abruptly, the silicon has diffused in the p side.

We showed that $Hg_{1-x}Cd_xTe$ junctions are possible in situ by MBE, but the control during the growth of the composition and the doping are very critical. In the near future heterojunctions will be attempted for gate control of FET channels. The R_oA values of the first homojunctions are still low compared to what is currently achieved on photodiodes. But we think that these results are very encouraging since the $Hg_{1-x}Cd_xTe$ material was not annealed and reflects the as-grown conditions very difficult to achieve, especially on the p-side.

For more detail see the attached paper accepted for publication in the Journal of Vacuum Science and Technology.

New achievements in $Hg_{1-x}Cd_xTe$ grown by molecular-beam epitaxy

S. Sivananthan, M. D. Lange, G. Monfroy, and J. P. Faurie
University of Illinois at Chicago, Department of Physics, Chicago, Illinois 60680

(Received 5 September 1987; accepted 14 December 1987)

A review of our recent achievements in the growth of $Hg_{1-x}Cd_xTe$ by molecular-beam epitaxy is presented here. The influences of the substrate temperature, the crystallographic orientation, and the nature of the substrate on the properties of $Hg_{1-x}Cd_xTe$ are discussed in detail. We show that to grow high-quality material with good uniformity in terms of the alloy composition and the doping by crystal stoichiometry deviation, the substrate temperature should be between 180 °C and T_{max}. We report mobilities as high as 5.0×120^5 $cm^2\,V^{-1}\,s^{-1}$ for n-type layers and 1.2×10^3 $cm^2\,V^{-1}\,s^{-1}$ for p-type layers, achieved by precisely controlling the growth parameters. We illustrate that the Hg condensation coefficient is influenced by the crystallographic orientation. Our results show that for $Hg_{1-x}Cd_xTe$ grown on both the (111)B and the (100) faces of CdTe or GaAs the Hall mobilities are very high and comparable. We report our important achievement of the successful growth of 2-in.-diam $Hg_{1-x}Cd_xTe$ films on GaAs(100), with $\Delta x/\bar{x}$ as low as 0.7% for $\bar{x}=0.218$ (Δx is the standard deviation and $\bar{x}$ is the mean value), $\Delta t/\bar{t}$ as low as 0.6% for the layer thickness, excellent uniformity in the doping, and high electron or hole mobility. This illustrates the excellent control that our group has achieved toward the growth of this material by molecular-beam epitaxy.

I. INTRODUCTION

Since 1981, important progress has been achieved toward the growth of $Hg_{1-x}Cd_xTe$ by molecular-beam epitaxy (MBE). The growth of high-quality epitaxial single layers and heterostructures is of vital interest for device technology. $Hg_{1-x}Cd_xTe$ is already the most important material for infrared technology, and is now appearing as a promising material for optical telecommunication systems.[1] The crystal quality along with the electrical performances of $Hg_{1-x}Cd_xTe$ epilayers grown by MBE have been greatly improved by careful control of the growth parameters. In terms of quality and electrical performance, MBE layers of $Hg_{1-x}Cd_xTe$ can now be compared with the best $Hg_{1-x}Cd_xTe$ grown by any other technique.

In this paper, we present a concise account of our recent achievements in the growth of $Hg_{1-x}Cd_xTe$ by MBE. The influence of various parameters such as the substrate temperature, the Hg flux, the crystallographic orientation and the nature of the substrate are discussed. The growth on 2-in.-diam GaAs substrates of $Hg_{1-x}Cd_xTe$ epilayers that are highly uniform in terms of alloy composition, mobility, and carrier concentration from doping by crystal stoichiometry deviation represents the best achievement ever reported for this material on such a large surface area and illustrates the excellent level of control that our group has reached in this difficult procedure. A brief summary of the results will be given here.

II. GROWTH ON CdTe(111)B SUBSTRATES

MBE compositional control is difficult to achieve for $Hg_{1-x}Cd_xTe$ due to the noncongruent reevaporation of this compound.[2] We have previously reported that reflected high-energy electron diffraction (RHEED) can be used to monitor the suitable Hg flux.[3] For a given Hg flux, a high-quality monocrystalline $Hg_{1-x}Cd_xTe$ film can be grown in the $(\bar{1}\bar{1}\bar{1})B$ orientation within a narrow substrate temperature range ($T_{max}-T_{min}$) of about 10 to 15 °C when the substrate temperature (T_s) is in the 180–190 °C temperature range. When T_s is below T_{min} the excess Hg desorbs, however, twins, which are detrimental for electrical performance, are observed. When growth occurs close to T_{min}, these growth defects might still exist on a longer periodicity range of 100 Å or more and consequently would not be easily detected by RHEED.[4] These defects are detrimental to the quality of the layer. When T_s is above T_{max} two possibilities exist. (1) If T_s is below 190 °C the excess Te leads to a polycrystalline material. (2) If T_s is above 195 °C the excess Te is reevaporated and the film still grows monocrystalline, but a change in composition is observed. Therefore, to grow high-quality $Hg_{1-x}Cd_xTe$ by MBE it is very important to control the Hg flux and the substrate temperature accurately and reproducibly from run to run, and uniformly over the sample. It should be pointed out that these parameters also play an important role in the doping of the film by crystal stoichiometry deviation. The growth rate, which has not yet been fully investigated, is also playing an important role in terms of crystal quality. A growth rate of about 4 Å s^{-1}, which represents the best compromise between the crystal characteristics and the growth duration of 10- to 15-μm-thick epilayers, is currently used.

Hg tends to evaporate preferentially from a $Hg_{1-x}Cd_xTe$ surface. It has been experimentally shown that the condensation coefficient for Hg is on the order of 10^{-3} for n-type $Hg_{1-x}Cd_xTe$ ($x\approx0.22$) grown in the (111)B orientation at a temperature 190 °C.[5] The condensation coefficient for a given element is defined as the ratio of the number of atoms incorporated in the layer to the number of atoms impinging the surface. As was pointed out already in 1982,[6] a temperature of 180 °C or more is required to grow high-quality $Hg_{1-x}Cd_xTe$ films by MBE along the (111)B direction. Therefore, a very high Hg flux is necessary to maintain epitaxial growth. To grow p-type $Hg_{1-x}Cd_xTe$ ($x\approx0.22$) with a growth rate of about 4 Å/s and a substrate temperature of

 0734-211X/88/020788-06$01.00

195 °C, about 1.5 cm^3 of Hg per micron layer is necessary in our system. This means that if a regular cell is used at a constant temperature, the Hg level would continuously change and would cause changes in the Hg flux which are unacceptable. This problem is solved by a continuous-feed Hg cell, such as the one we are currently using.

It has been previously reported that the composition (x) is primarily controlled by the Cd to Te flux ratio. This is correct when the Hg flux is roughly constant from one growth to the next and the substrate temperature is in the 180–190 °C range. We have investigated the influence of substrate temperature on the composition. $Hg_{1-x}Cd_xTe$ layers that were grown at different substrate temperatures, but with the same fluxes. The thicknesses and the compositions are obtained by infrared transmission spectroscopy at room temperature. For each, the cutoff wavelength is defined as that for which the absorption coefficient (α) is equal to 500 cm^{-1}. The formula for the absorption coefficient is $\alpha = -\ln(\text{transmittance})/\text{thickness}$. This method has been proven to provide band gap measurements which are in good agreement with those determined from the temperature dependence of the R_0A products of diodes.[7] The thicknesses of the layers are calculated from the interference peak spacings on the infrared transmission spectra. A large change in the transmission spectrum was observed between the layers grown at 205 and 213 °C, while a smaller but not negligible change was observed between those grown at 200 and 205 °C (Fig. 1). In a different experiment carried out at temperatures 185 and 200 °C no changes in the growth rate, and consequently composition were observed between 185 and 195 °C (Table I). Due to the large change in the condensation coefficient of Hg with temperature, it is impossible to carry out one set of experiments for the entire temperature range. Comparing changes in the composition and the growth rate, one can see that these are both caused by a change in the growth rate of HgTe, but not of CdTe (Table I). The composition remains constant for substate temperatures between 185 and 195 °C showing that the condensation coefficient of Te is constant for the given Hg flux. When the substrate temperature is above 204 °C, which is the maximum substrate temperature for given Hg flux, the rapid re-

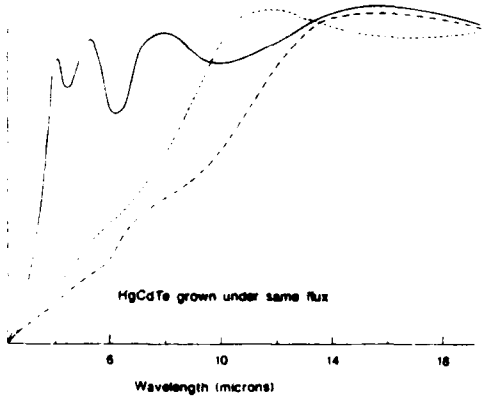

FIG. 1. Infrared transmission spectroscopic measurements of $Hg_{1-x}Cd_xTe$ grown with the same fluxes, but at different temperatures. — = 210 °C; - - - = 205 °C; -·- = 200 °C.

TABLE I. Comparison of growth rates and the x values for layers grown with the same fluxes but different substrate temperatures.

Substrate temperature (°C)	Composition (x)	Growth rate (Å/s)	Relative growth rate of CdTe (Å/s)	Relative growth rate of HgTe (Å/s)
185[a]	...	...	...	4.39
195[a]	...	...	...	4.40
200	0.17	5.17	0.88	4.29
205	0.19	4.67	0.89	3.78
213	0.31	2.78	0.86	1.92

[a] Extrapolated from a separate experiment.

vaporation of Hg leaves free Te which is also reevaporated and the film still grows monocrystalline. But an increase in the x value of 1.5% to 2% for each 1 °C increase in the substrate temperature is observed, along with a large change in the growth rate. This problem could be partially solved by increasing the Hg flux.

It is important to recall that a change in x of only $\Delta x = \pm 0.0015$ is the objective to reach for infrared detection devices operating at a cutoff wavelength of 10 μm at 77 K. It is obvious that such a requirement cannot be achieved if part of the substrate temperature is above T_{max}. Now if the substrate temperature is between T_{max} and T_{min} (incidently the T_{max} and T_{min} values are changing over the substrate since the Hg flux distribution is not constant) the epilayers will still experience a change in the doping level and even in the conduction type.

Stability in the temperature, with variations much less than $\pm$ 0.5 °C during the growth can be achieved. But, uniformity in the temperature with variations $< \pm 0.5$ °C over large surface areas has not yet been demonstrated. Consequently, taking into consideration the need of high-quality material with excellent uniformity in the composition, the substrate temperatures used should be between 180 °C and T_{max}. Also, to grow $Hg_{1-x}Cd_xTe$ with good uniformity in the composition and the carrier concentration over the substrate, it is important to achieve a very low temperature gradient and to control precisely the substate temperature in the 180 °C–T_{max} range. In addition, a reproducibility of the substrate temperature within 1 °C should be achieved in order to produce both the composition and the carrier concentration desired from run to run.

Such control will be fruitless if the Hg, Cd, and Te fluxes are not very constant. The Cd and Te fluxes are precisely controlled through the temperatures of the effusion cells which are stable within 0.2 °C. The Hg flux, which has lesser importance than the Cd and Te fluxes in controlling of the composition, is monitored by an ion gauge and kept constant within a range of fluctuation of $< 10\%$. This represents cell temperature fluctuations of < 0.5 °C.

Gradients in the substate temperature and the fluxes (the latter due to the cosine distributions of the fluxes) increase with the size of the substrate. Therefore, it becomes obvious that MBE growth of $Hg_{1-x}Cd_xTe$ on large area 2-in. diameter or greater substrates, uniform both in composition and carrier concentration, represents a real challenge. The need

for rotation of the substrate becomes unavoidable because the alternative of using cell-to-substrate distances of about one meter is unacceptable in terms of Hg consumption. Rotation of the substrate, however, hinders proper mechanical contact between the thermocouple and the substrate holder. (Such use of a thermocouple is normally a convenient way to control the temperature of the surface, although not reliably accurate in case of sudden change of the surface temperature.) Therefore a pyrometer must be used.

III. THE INFLUENCE OF THE CRYSTALLOGRAPHIC ORIENTATION

In MBE a nonequilibrium situation is intentionally introduced to drive the system to form a solid from the vapor phase by adjusting the substrate temperature and the partial pressures of the molecular fluxes. The formation of epitaxial layers is highly influenced by the mass transport and the crystal surface. Therefore the crystallographic orientation can play a major role in the growth and properties of $Hg_{1-x}Cd_xTe$ grown by MBE.

The influence of the crystallographic orientation on condensation coefficients has been compared among the (111)*A*, (111)*B*, and (100) orientations. In each case the $Hg_{1-x}Cd_xTe$ growth was closely followed by RHEED. The minimum amount of Hg necessary to maintain the growth was determined by slowly decreasing the Hg flux until difficulties in maintaining monocrystalline growth were observed. As we have reported[8] before, with all the other conditions including the composition kept constant, the minimum amount of Hg necessary to maintain epitaxial growth of $Hg_{1-x}Cd_xTe$ at 185 °C is almost an order of magnitude higher for the (111)*A* orientation than for the (111)*B* orientation. The minimum amount of Hg necessary to maintain epitaxial growth along the (100) orientation falls in between that for the (111)*A* and the (111)*B* orientations. These results can be explained in terms of the bonding of surface atoms. Hg atoms are more well protected from reevaporation in the (111)*B* orientation than the (100) orientation, and have the least protection in the (111)*A* orientation. A similar but less dramatic tendency is observed for Cd.

Results regarding the growth parameters for different orientations provide an important means for ascertaining the best orientation for growth. From a Hg consumption point of view, one could conclude that the (111)*B* orientation is the best. But it is important that other parameters, such as the quality of the layer and the ease of control of the doping by stoichiometry deviation, are taken into consideration before coming to a conclusion. For the (111)*A* orientation, growth by MBE of a high-quality CdTe buffer layer with a low-defect density is very difficult. Moreover, the amount of Hg needed to maintain the epitaxial growth of $Hg_{1-x}Cd_xTe$ for the (111)*A* orientation is about ten times that for the (111)*B* orientation. This huge amount of Hg needed for the (111)*A* orientation growth creates a major problem for the ultrahigh vacuum (UHV) of the MBE system. Therefore, the (111)*A* orientation is not suitable for MBE growth of $Hg_{1-x}Cd_xTe$. For this reason we have investigated only the (111)*B* and the (100) orientations.

On the other hand the (111)*B* orientation has a major disadvantage for the control of the growth of high-quality layer. That is stacking faults, which are often observed on the (111)*B* face. When the Hg flux is too high, twining effects which are caused by antiphase domains are observed. This implies that the twining process occurs very easily along this direction. This problem is in fact often observed for zinc-blende crystals grown in the (111) orientation, but the growth of pyramids has been observed when the growth conditions are not well controlled.[4] No such phenomenon is observed for the (100) orientation. Samples for which twins are observed by RHEED during growth exhibit high-carrier concentration and low mobility. Also, electroreflectance measurements carried out on some (111)*B* orientation $Hg_{1-x}Cd_xTe$ layers have shown an increase in the line width (Γ) on such films.[10] For the (100) orientation, even though more Hg is necessary to grow $Hg_{1-x}Cd_xTe$ no such defects are observed. Thus the growth seems to be more easy to control in the (100) orientation than in the (111)*B* orientation. It should be pointed out that *n*-type $Hg_{1-x}Cd_xTe$ can easily be grown along the (100) orientation even for $x > 0.30$, while *p*-type $Hg_{1-x}Cd_xTe$ is easily grown in the (111)*B* orientation for $x > 0.19$. This experimental result is difficult to understand if one considers that the *p*-type characteristic is associated with Hg vacancies because then (100) layers should be more *p*-type than (111)*B* layers since the Hg condensation coefficient is lower on the (100) face. We are currently investigating this problem.

Table II shows a comparison of the best Hall data of *n*-type samples grown either in the (100) or the (111)*B* surface. These values indicate that the mobilities are very much comparable for the two crystallographic orientations. The electron mobility of 5.0×10^5 cm^2 V^{-1} s^{-1} for $Hg_{1-x}Cd_xTe$ grown on the (111)*B* face, is close to the theoretical limit of the electron mobility in HgCdTe with this Cd concentration. Often, $Hg_{1-x}Cd_xTe$ grown on the (100) surface has a higher electron mobility than that on the (111)*B* surface. This shows that the control of the growth parameters for $Hg_{1-x}Cd_xTe$ grown by MBE is more critical for the (111)*B* orientation than the (100) orientation.

Table III compares the hole mobility of $Hg_{1-x}Cd_xTe$ grown on the (100) and the (111)*B* surfaces. It is important to point out that these high-hole mobilities have been obtained for epilayers which have no small HgTe layer at the interface with the substrate (we have shown that the presence of HgTe at that interface can enhance hole mobility).[10] The hole mobility of 1.2×10^3 cm^2 V^{-1} s^{-1} observed in a (111)*B* orientation is higher than the best *p*-type mobility of 5.1×10^2 cm^2 V^{-1} s^{-1} for layers grown on the (100) surface. It should be pointed out that we do not have as much data for *p*-type $Hg_{1-x}Cd_xTe$ grown on the (100) surface. Therefore, it would be premature to draw a final conclusion for hole mobilities.

Since the (100) surface requires more Hg than the (111)*B* surface, then from both the UHV and the economic points of view, the (111)*B* orientation is the best. As for the growth point of view, we suggest that high-quality *n*-type $Hg_{1-x}Cd_xTe$ layers are more easily grown along the (100) orientation [more has to be understood about the *n*-type

TABLE II. Electrical characteristics of *n*-type HgCdTe grown by MBE between 180 and 190 °C.

Sample	Composition x	Thickness	Orientation	Carrier conc. $N_D - N_A$ (cm^{-3}) at 300 K	Mobility μ_H ($cm^2 V^{-1} s^{-1}$) at 300 K	T	Carrier conc. $N_D - N_A$ (cm^{-3})	Mobility μ_H ($cm^2 V^{-1} s^{-1}$)
				CdTe substrate				
241-600	0.18	8.0 μm	(100)	1.3×10^{17}	3.0×10^{4}	20 K	4.2×10^{15}	3.7×10^{5}
214-526	0.19	11.7 μm	(111)*B*	4.6×10^{16}	1.6×10^{4}	20 K	2.5×10^{14}	3.1×10^{5}
7-233(82)	0.20	6.0 μm	(111)*B*	4.0×10^{16}	1.7×10^{4}	77 K	2.0×10^{15}	1.9×10^{5}
162-431	0.22	2.0 μm	(100)	2.0×10^{16}	2.0×10^{4}	77 K	6.0×10^{15}	1.6×10^{5}
				CdZnTe substrate				
32-598	0.18	8.6 μm	(111)*B*	1.1×10^{17}	1.0×10^{4}	20 K	9.9×10^{14}	2.1×10^{5}
19-405	0.20	9.0 μm	(111)*B*	3.1×10^{16}	1.4×10^{4}	77 K	2.0×10^{15}	1.2×10^{5}
				GaAs substrate				
576-396	0.18	2.7 μm	(111)*B*	1.0×10^{17}	1.9×10^{4}	30 K	1.5×10^{15}	5.0×10^{5}
12- 17	0.19	6.2 μm	(100)	1.0×10^{17}	2.4×10^{4}	30 K	1.0×10^{16}	2.4×10^{5}
403-250	0.20	1.0 μm	(100)	5.0×10^{16}	1.5×10^{4}	40 K	1.0×10^{16}	3.0×10^{5}
191-102	0.22	1.0 μm	(111)*B*	2.0×10^{16}	1.1×10^{4}	50 K	4.0×10^{15}	1.0×10^{5}

doping in (100)], while high-quality *p*-type $Hg_{1-x}Cd_xTe$ layers are more easily obtained by growing along the (111)*B* orientation. Therefore provided that a good control of the growth parameters is achieved, what actually can be done, (111)*B* seems to be the best orientation.

IV. GROWTH ON GaAs(100) SUBSTRATES

The growth of high-quality epitaxial films is limited by the substrate quality. CdTe, because of its closeness in lattice parameter and its metallurgical compatibility with $Hg_{1-x}Cd_xTe$, is a natural choice for the substrate material. However, the lack of availability of high-structural perfection CdTe substrates has stimulated interest in growth of $Hg_{1-x}Cd_xTe$ by MBE on other substrates. X-ray rocking curves measured on samples grown on CdTe, and CdZnTe substrates indicate that comparable crystalline qualities can be reached, but the nonhomogeneity of the substrates appears to be the primary limiting factor. Large dispersions in full widths at half-maximum (FWHM) are currently observed on commercially available CdTe or CdZnTe substrates. Nevertheless, it is important to point out that when the growth conditions are under good control and the substrates of high quality, HgCdTe epilayers can almost duplicate the crystal quality of substrates. As an illustration, FWHM as low as 17 and 18 arcsec (Fig. 2) were recorded on samples grown on CdTe and CdZnTe. Nevertheless when

TABLE III. Electrical characteristics of *p*-type HgCdTe grown by MBE between 190 and 200 °C (no HgTe layer at the interface).

Sample	Substrate	Composition x	Thickness	Carrier conc. $N_D - N_A$ (cm^{-3}) at 300 K	Mobility μ_H ($cm^2 V^{-1} s^{-1}$) at 300 K	T	Carrier conc. $N_A - N_D$ (cm^{-3})	Mobility μ_H ($cm^2 V^{-1} s^{-1}$)
				(111)*B* orientation				
196-481	CdTe	0.20	4.8 μm	1.6×10^{16}	9.0×10^{3}	30 K	6.0×10^{15}	1.1×10^{3}
198-484	CdTe	0.21	4.3 μm	2.9×10^{16}	8.5×10^{3}	30 K	5.1×10^{15}	1.0×10^{3}
242-602	CdTe	0.22	11.9 μm	2.1×10^{16}	8.4×10^{3}	23 K	2.0×10^{15}	1.1×10^{3}
215-527	CdTe	0.25	11.9 μm	5.8×10^{15}	7.5×10^{3}	30 K	6.2×10^{15}	8.7×10^{2}
205-516	CdTe	0.29	15.6 μm	3.0×10^{15}	4.5×10^{3}	30 K	7.5×10^{15}	8.7×10^{2}
216-528	CdTe	0.34	12.1 μm	1.6×10^{16}	1.5×10^{2}	77 K	3.6×10^{15}	8.0×10^{2}
667-532	GaAs	0.20	2.1 μm	2.4×10^{16}	1.0×10^{4}	23 K	4.1×10^{15}	1.2×10^{3}
681-540	GaAs	0.21	3.7 μm	2.4×10^{16}	1.0×10^{4}	23 K	3.6×10^{15}	1.1×10^{3}
583-453	GaAs	0.22	5.4 μm	1.8×10^{16}	6.7×10^{3}	30 K	1.4×10^{15}	8.7×10^{2}
654-508	GaAs	0.25	3.8 μm	6.2×10^{15}	4.5×10^{3}	30 K	1.1×10^{16}	7.3×10^{2}
393-244	GaAs	0.28	1.3 μm			40 K	2.8×10^{15}	5.2×10^{2}
500-308	GaAs	0.31	2.3 μm	2.6×10^{15}	2.4×10^{3}	30 K	1.1×10^{15}	4.5×10^{2}
4-319	CdTeSe	0.31	7.6 μm	3.1×10^{15}	3.2×10^{3}	30 K	2.4×10^{15}	8.4×10^{2}
2-310	CdTeSe	0.32	9.4 μm	2.1×10^{15}	1.9×10^{3}	30 K	1.2×10^{15}	6.7×10^{2}
34-605	CdZnTe	0.24	9.2 μm	8.6×10^{15}	5.7×10^{3}	23 K	1.4×10^{15}	8.0×10^{2}
				(100) orientation				
673-534	GaAs	0.21	4.2 μm	2.0×10^{16}	4.6×10^{3}	23 K	3.4×10^{15}	5.1×10^{2}
125-304	CdTe	0.24	3.0 μm	4.1×10^{15}	3.6×10^{3}	77 K	2.0×10^{16}	2.5×10^{2}
127-306	CdTe	0.29	2.7 μm	4.1×10^{15}	2.9×10^{3}	77 K	1.5×10^{16}	1.2×10^{2}

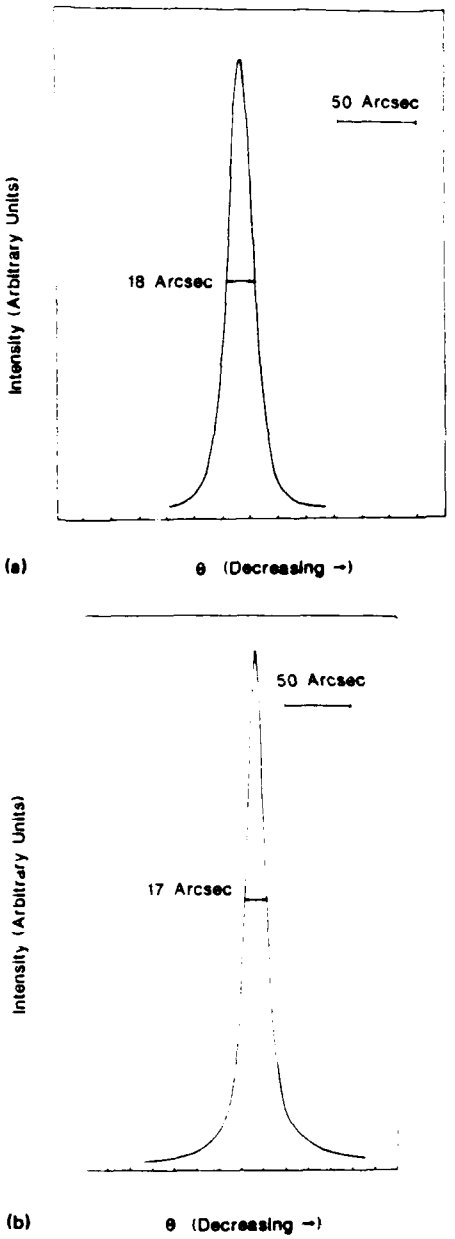

FIG. 2. X-ray rocking curve recorded along the (333) direction, using the Cu-K_α line ($\lambda = 1.540562$ Å). (a) HgCdTe on CdTe substrate. Sample #242602, reflection (333). (b) HgCdTe on CdZnTe substrate. Sample #38617, reflection (333).

the x-ray probe was moved the half-width deteriorated due to the lack of uniformity of the substrates. The lack of availability of tellurium-based substrates makes GaAs very attractive. The interest in growing $Hg_{1-x}Cd_xTe$ on GaAs still exists, despite the important progress made in the improvement of CdTe crystal quality during this last year, because CdTe and related materials are much more expensive than GaAs and not available in 2- and 3-in.-diam sizes. Thus it is interesting to update constantly the data obtained for epilayers grown on these different substrates. Electron and hole mobility, and carrier concentration are chosen for such comparison because such characterization is closely related to device characteristics.

Much discussion has occurred regarding the epitaxy of CdTe on GaAs(100) since both (111)*B* and (100) oriented CdTe can be grown on GaAs(100).[11-15] It has been recently shown that (111)*B* orientation and (100) orientation CdTe grown on GaAs(100) are of high quality, but also that the quality of the (100) CdTe improves when the oxide is totally desorbed prior to growth. In order to completely desorb the oxide the GaAs should be preheated to 580 °C. However, this creates an As deficient surface. Therefore, to grow (100) CdTe. either the substrate should be preheated to 580 °C under As or Te flux, or first $Cd_{1-x}Zn_xTe$ with $x > 0.15$ should be grown after preheating to 580 °C. The growth of $Hg_{1-x}Cd_xTe$ on CdTe//GaAs(100) substrate has been previously reported.[16] Electron diffraction patterns obtained during such growth attest to the high quality of these films. The observation of an electron mobility as high as 5.0×10^5 cm^2 V^{-1} s^{-1} for $Hg_{1-x}Cd_xTe$ (111)*B* grown on GaAs indeed indicates that the quality of such layers is excellent. Tables II and III display and compare electrical characteristics of *n*-type and *p*-type $Hg_{1-x}Cd_xTe$ epilayers grown on various substrates. Using mobility as a tool to compare the quality of these layers, one could conclude that $Hg_{1-x}Cd_xTe$ grown on GaAs(100) substrates is of high quality, comparable to that grown on CdTe, CdZnTe, and CdTeSe. Of course finally the comparison of IR devices made from $Hg_{1-x}Cd_xTe$ layers grown on different substrates will provide the ultimate test.

V. GROWTH ON 2-IN.-DIAM GaAs(100) SUBSTRATES

As discussed above, the growth of $Hg_{1-x}Cd_xTe$ on 2-in.-diam GaAs(100) substrates represents a real challenge since all the growth parameters must be extremely well controlled. But certainly success in this endeavor will be an important achievement for $Hg_{1-x}Cd_xTe$ detector technology. Several 2-in.-diam $Hg_{1-x}Cd_xTe$ layers have been grown on GaAs(100). All of them exhibit uniform mirrorlike surfaces. The details of the growth and characterization are given elsewhere.[17] In order to determine the uniformity in thickness composition, infrared transmission measurements have been performed at several positions on the samples. A standard deviation ($\Delta x/x$) as low as 0.7% of the mean composition ($\bar{x}$) and likewise a measurement for $\Delta t/\bar{t}$ of 0.6% for the thickness have been observed for 5-μm-thick layers with composition around 0.22.

For a *p*-type film grown on the (111)*B* surface the carrier concentration ($N_a - N_d$) increased by a factor of 2 from 3.6×10^{15} cm^{-3} at the center to 7.2×10^{15} cm^{-3} at the edge of the film, while the hole mobility increased from 5.7×10^2 cm^2 V^{-1} s^{-1} at the center to 6.2×10^2 cm^2 V^{-1} s^{-1} at the edge. A 2-in.-diam *n*-type $Hg_{1-x}Cd_xTe$ film was grown on the (100) surface. For this film mobility varied between 1.3×10^5 cm^2 V^{-1} s^{-1} and 1.8×10^5 cm^2 V^{-1} s^{-1} indicating a layer of good quality. Also for this *n*-type layer the carrier concentration ($N_d - N_a$) ranged only from 4.0×10^{15} to 4.4×10^{15} cm^{-3}, exhibiting extreme uniformity.

VI. CONCLUSION

In this paper we have presented recent achievements in the growth of $Hg_{1-x}Cd_xTe$. We have shown that in order to grow high quality, homogeneous, thick $Hg_{1-x}Cd_xTe$ epilayers of large area the substrate temperature should not be lower than 180 °C or higher than T_{max}. We have discussed the role of the crystallographic orientation in terms of the Hg condensation coefficient and the control of the conduction type [*n*-type $Hg_{1-x}Cd_xTe$ films can easily be grown in the (100) orientation, whereas *p*-type $Hg_{1-x}Cd_xTe$ layers are easily grown in the (111)*B* orientation]. Electrical measurements show that when the growth parameters are well controlled, the quality of $Hg_{1-x}Cd_xTe$ grown in both the (111)*B* and the (100) orientations is comparable, thus giving the advantage to the (111)*B* growth direction which requires less mercury. We confirm that $Hg_{1-x}Cd_xTe$ layers grown on GaAs substrates are electrically as good as those grown on CdTe, CdZnTe or CdTeSe substrates. We have shown that high-quality $Hg_{1-x}Cd_xTe$ films of 2-in.-diam can be grown. High-Hall mobilities, uniform thicknesses, and very uniform compositions have been achieved already in these films. Further improvements in the temperature uniformity of the samples, along with increased uniformity of the Hg flux on the samples is expected to improve the uniformity of $Hg_{1-x}Cd_xTe$ layers with even larger surface areas. These results represent important achievements toward the use of $Hg_{1-x}Cd_xTe$ layers grown by MBE for infrared detector technology.

ACKNOWLEDGMENTS

The authors would like to thank P. S. Wijewarnasuriya, I. K. Sou, X. Chu, and M. Boukerche for their assistance, and S. Farook and Z. Ali for the technical assistance. This work was supported by DARPA and monitored by Air Force Office of Scientific Research under Contract No. F49620-87-C-0021.

[1] C. Verie, F. Raymond, and G. Neu, J. Vac. Sci. Technol. B **4** (1986).
[2] R. F. C. Farrow, C. R. Jones, G. M. Williams, P. W. Sullivan, W. J. O. Boyle, and J. T. M. Wotherspoon, J. Phys. D **12**, L117 (1979).
[3] J. P. Faurie, J. Reno, S. Sivananthan, I. K. Sou, X. Chu, M. Boukerche, and P. S. Wijewarnasuriya, J. Vac. Sci. Technol. B **4**, 585 (1986).
[4] R. D. Horning and J. L. Stauderman, Appl. Phys. Lett. **49**, 1590 (1986).
[5] J. P. Faurie and A. Million, J. Cryst. Growth **54**, 582 (1981).
[6] J. P. Faurie and A. Million, Appl. Phys. Lett. **41**, 264 (1982).
[7] J. P. Faurie, S. Sivananthan, M. Lange, R. F. Dewames, A. M. B. Vandewyck, G. M. Williams, Dan Yamini, and E. Yao, Appl. Phys. Lett. (submitted).
[8] S. Sivananthan, X. Chu, J. Reno, and J. P. Faurie, J. Appl. Phys. **60**, 1359 (1986).
[9] P. M. Raccah, J. W. Garland, Z. Zhang, A. H. M. Chu, J. Reno, I. K. Sou, M. Boukerche, and J. P. Faurie, J. Vac. Sci. Technol. A **4**, 2077 (1986).
[10] J. P. Faurie, I. K. Sou, D. Rafol, and K. C. Woo, Phys. Rev. B **34**, 6000 (1986).
[11] J. P. Faurie, C. Hsu, S. Sivananthan, and X. Chu, Surf. Sci. **168**, 473 (1986).
[12] J. M. Ballingall, M. L. Wroge, and D. J. Leopold, Appl. Phys. Lett. **48**, 1273 (1986).
[13] L. A. Kolodzieski, R. L. Gunshor, N. Otsuka, X. C. Zhang, S. K. Chang, and A. V. Nurmikko, Appl. Phys. Lett. **47**, 882 (1985).
[14] R. N. Bickness, R. Y. Yanka, N. C. Giles, J. F. Schetzina, T. Z. Nagee, C. Leung, and H. Hawayoshi, Appl. Phys. Lett. **44**, 363 (1984).
[15] P. P. Chow, L. A. Greenlaw, and D. Johnson, J. Vac. Sci. Technol. A **1**, 562 (1983).
[16] J. P. Faurie, S. Sivananthan, M. Boukerche, and J. Reno, Appl. Phys. Lett. **45**, 1307 (1984).
[17] M. D. Lange, S. Sivananthan, X. Chu, and J. P. Faurie, Appl. Phys. Lett. (to be published).

Molecular beam epitaxial growth and characterization of 2-in.-diam $Hg_{1-x}Cd_xTe$ films on GaAs (100) substrates

M. D. Lange, S. Sivananthan, X. Chu, and J. P. Faurie
University of Illinois at Chicago, Department of Physics, P. O. Box 4348, Chicago, Illinois 60680

(Received 21 October 1987; accepted for publication 25 January 1988)

$Hg_{1-x}Cd_xTe$ films with 2 in. diameters have been grown by molecular beam epitaxy on GaAs (100) substrates. These films were grown in both the (100) and ($\overline{1}\overline{1}\overline{1}$)*B* crystallographic orientations and in both conduction types. They were characterized by *in situ* electron diffraction, infrared absorption, and van der Pauw dc Hall measurements. Their surfaces were shiny and mirrorlike from center to edge. The Cd concentrations (x) of these films were very uniform, exhibiting standard deviations (Δx) as low as 0.7% of the mean ($\bar{x}$). Their thicknesses also were uniform within 0.6%. These films were completely uniform in their conduction types; that is, the *n*-type films were entirely *n* type, and likewise for the *p*-type films. The Hall mobilities of these films show them to be of high quality, with values as high as 6.7×10^2 cm^2 V^{-1} s^{-1} for the *p*-type ($x=0.22$) and 1.8×10^5 cm^2 V^{-1} s^{-1} for the *n*-type films ($x=0.21$). These results represent an important achievement toward the future of infrared detector technology.

$Hg_{1-x}Cd_xTe$ is the most important material for infrared detectors and imaging arrays, and has promise for applications in fiber-optic telecommunication systems. This is primarily due to the fact that the band gap for $Hg_{1-x}Cd_xTe$ is a function of the Cd concentration (x) as well as the ambient temperature (T). There are two main windows in the atmosphere of the earth with wavelengths in the 3–5 μm and 8–14 μm regions, while fiber-optic telecommunication systems currently operate in the 1.3–1.6 μm range. Control of the x value during growth of $Hg_{1-x}Cd_xTe$ tailors the band gap to fall into the energy ranges for all these wavelength regions.

As the molecular beam epitaxial (MBE) growth technique has continued to improve for $Hg_{1-x}Cd_xTe$ epilayers, the prospects for films of larger area have begun to be explored. These larger area films are important for imaging arrays and will be especially vital in the future for the efficient production of $Hg_{1-x}Cd_xTe$ material. The growth by MBE of a uniform $Hg_{1-x}Cd_xTe$ film on a large substrate is very difficult to achieve because of the nonuniform distribution of the fluxes and nonuniform temperature of the substrate. The cosine distribution of the fluxes is usually encountered in the MBE growth of III-V compounds, and its consequences are (1) thickness variation over the wafer, (2) change in composition for an alloy with more than two elements, and (3) change in the doping level when an electrically active impurity is evaporated at the same time (the doping in III-V compounds is not controlled by stoichiometry deviation). In the case of $Hg_{1-x}Cd_xTe$ a simple cosine distribution is expected for the Cd and Te fluxes, but due to the high effusion rate required for Hg the expected Hg flux distribution has the behavior of $\cos^{3/2}\theta$, where θ is measured from the axis of the Hg effusion cell[1]. Therefore, with this more forward directional Hg flux the nonuniformity in thickness and composition currently observed in the growth by MBE of semiconducting alloys should be worse in the case of $Hg_{1-x}Cd_xTe$. In addition to that, since the conduction type and the carrier concentration can be controlled by stoichiometry deviation during the growth of $Hg_{1-x}Cd_xTe$ by MBE, these spatial flux variations will also have an effect on the electrical properties of the layers.

Above all however, there is the problem due to the exponential change of the Hg condensation coefficient with temperature. We have shown that for a given Hg flux, a high-quality monocrystalline $Hg_{1-x}Cd_xTe$ film can be grown in the ($\overline{1}\overline{1}\overline{1}$)*B* orientation within a narrow substrate temperature range ($T_{max}-T_{min}$) of about 10–15 °C when the substrate temperature (T_s) is in the 180–190 °C temperature range.[2] When T_s is below T_{min} the excess Hg desorbs, but twins, which are detrimental for electrical performance, are observed. When T_s is above T_{max} two possibilities exist. (1) If T_s is below 190 °C the excess Te leads to a polycrystalline material. (2) If T_s is above 195 °C the excess Te is reevaporated and the film still grows monocrystalline, but an increase in the x value of 1.5–2% for each 1 °C increase in the substrate temperature is observed, along with a large change in the growth rate.[3]

It is important to recall that a change in x of only $\Delta x = \pm 0.001$ is the goal to reach for infrared detection devices operating at a cutoff wavelength of 10 μm at 77 K. It is obvious that such a requirement cannot be achieved if part of the substrate temperature is above T_{max}. Now if the substrate temperature is between T_{max} and T_{min} (incidentally the T_{max} and T_{min} values are changing over the substrate since the Hg flux distribution is not constant) the epilayers will still experience a change in the doping level and even in the conduction type.

To minimize these temperature variations the substrate must be rotated during the growth, but this also hinders the precise temperature measurement of the substrate by a thermocouple. In order to have adequate control of the temperature during the growth, the use of an infrared pyrometer, which can give reproducible results, has been employed.

The combination of flux distribution and substrate temperature variation makes the growth by MBE of large high-quality uniform $Hg_{1-x}Cd_xTe$ films a real challenge.[4] For the first time we report here 2-in.-diam $Hg_{1-x}Cd_xTe$ films, both *p*-type and *n*-type, grown by MBE, which exhibit uni-

 0003-6951/88/120978-03$01.00

form x values and high mobilities.

The 2-in.-diam $Hg_{1-x}Cd_xTe$ films were grown in the ultrahigh vacuum of a Riber 2300 MBE machine modified to handle Hg. In this machine the substrate is situated to face an array of effusion cells containing CdTe, Te, and Hg. The temperatures of these cells and the substrate are precisely controlled to achieve proper growth conditions. The sample manipulator is designed to allow for rotation of the sample in the plane of its surface. This feature was exploited for the growth of the 2-in.-diam $Hg_{1-x}Cd_xTe$ films to achieve higher uniformity.

The substrates used for growing these 2-in.-diam films were high-quality prepolished GaAs (100) wafers. The chemical and *in situ* cleaning procedures used for these were the same as those discussed elsewhere[2] for the preparation of GaAs surfaces. Prior to growing the $Hg_{1-x}Cd_xTe$ films, buffer layers of CdTe were grown on the GaAs substrates. There is a 14.6% lattice mismatch between GaAs and $Hg_{1-x}Cd_xTe$. Therefore, to avoid a high dislocation density in the $Hg_{1-x}Cd_xTe$ films, the CdTe buffer layers are grown to a thickness of roughly 2.5 μm. As has been previously reported,[5,6] these CdTe buffer layers may be grown in either the (100) or the $(\overline{1}\overline{1}\overline{1})B$ crystallographic orientation.

Several 2-in.-diam $Hg_{1-x}Cd_xTe$ films of each conduction type were grown in both the (100) and the $(\overline{1}\overline{1}\overline{1})B$ orientations. In an earlier article[7] it was shown that the minimum Hg flux required for successful growth differs for these two orientations. Growth in the (100) orientation requires a higher flux than that in the $(\overline{1}\overline{1}\overline{1})B$ orientation. The Hg flux in combination with the substrate temperature used for the growth of $Hg_{1-x}Cd_xTe$ determines the crystal stoichiometry deviation, and thus the conduction type. The substrate temperatures chosen for the growth of the films reported here were 190 °C for the p-type and 185 °C for the n-type film, and the Hg flux used for the n-type film was higher than that used for the p-type film. We report here the data from one representative film of each conduction type.

The p-type film reported here was grown in the $(\overline{1}\overline{1}\overline{1})B$ orientation, while the orientation for the reported n-type film was (100). The films exhibited uniform mirrorlike surfaces, as illustrated by the photograph in Fig. 1. In order to ascertain the uniformity of each $Hg_{1-x}Cd_xTe$ film over its 2-in.-diam surface area, infrared transmission and van der

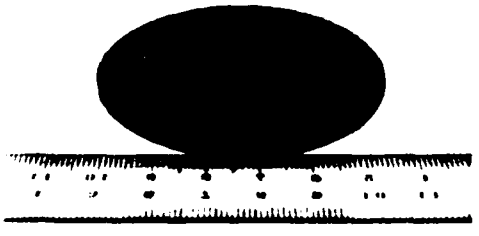

FIG. 1. Two-in. $Hg_{1-x}Cd_xTe$ film, grown by MBE on a CdTe/GaAs substrate.

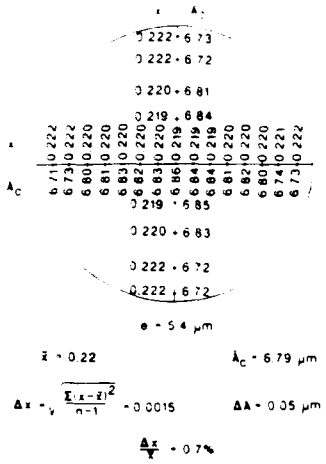

FIG. 2. Infrared transmission measurements at 300 K for 2-in.-diam $Hg_{1-x}Cd_xTe$ (111) film grown at 190 °C on a CdTe (111)/GaAs (100) substrate. Sample No. 583453. λ_c = cutoff wavelength; x = Cd concentration; e = thickness of $Hg_{1-x}Cd_xTe$ film.

Pauw dc Hall measurements were performed at several positions. The infrared transmission spectra were measured at room temperature. The cutoff wavelengths were in the 6–8 μm region. The cutoff wavelength is defined as that for which the absorption coefficient is $\alpha = -\ln$ (transmittance)/thickness. From the measured cutoff wavelengths for each position on the 2-in.-diam $Hg_{1-x}Cd_xTe$ films, the Cd concentrations (x) were calculated using the relation of Hansen *et al.*[8] Also, from the interference spacing in the infrared transmission spectra the thickness at each position on these films was determined.

For the p-type film reported here the uniformity of the x value proved to be excellent, as illustrated in Fig. 2. The average value of x (denoted by $\bar{x}$) was 0.22, while the standard deviation $\{\Delta x = [\Sigma(x-\bar{x})^2/n-1]^{1/2}\}$ was 0.0015, giving as a measure of the composition uniformity $\Delta x/\bar{x} = 0.7\%$. This is an excellent result since the goal required for infrared detectors in terms of composition uniformity is

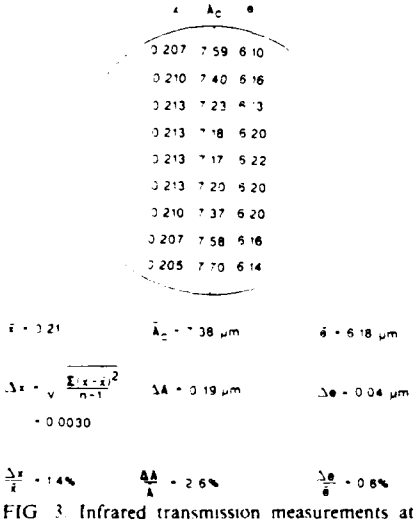

FIG. 3. Infrared transmission measurements at 300 K for 2-in.-diam $Hg_{1-x}Cd_xTe$ (100) film grown at 185 °C on a CdTe (100)/GaAs (100) substrate. Sample No. 750576. λ_c = cutoff wavelength; x = Cd concentration; e = thickness of $Hg_{1-x}Cd_xTe$ film.

TABLE I. Hall measurements at $B = 0.2$ T for 2-in.-diam $Hg_{1-x}Cd_xTe$ (111) film grown at 190 °C on CdTe (111)/GaAs (100) substrate. Sample No. 583453. $x = 0$, $y = 0$ is at the center of the sample.

x (mm)	y (mm)	Cond. type	300 K $N_d - N_a$ (cm^{-3})	300 K μ_H ($cm^2 V^{-1} s^{-1}$)	T(K) when $R_H = 0$	Cond. type	40 K $N_a - N_d$ (cm^{-3})	40 K μ_H ($cm^2 V^{-1} s^{-1}$)
0	0	n	2.1×10^{16}	6.4×10^3	90	p	3.6×10^{15}	5.7×10^2
4	0	n	2.0×10^{16}	5.0×10^3	90	p	3.0×10^{15}	5.2×10^2
7	0	n	2.1×10^{16}	6.3×10^3	90	p	4.7×10^{15}	5.5×10^2
11	0	n	1.9×10^{16}	6.2×10^3	90	p	5.1×10^{15}	5.7×10^2
15	0	n	1.9×10^{16}	6.8×10^3	90	p	5.6×10^{15}	6.5×10^2
18	0	n	1.8×10^{16}	6.8×10^3	90	p	7.2×10^{15}	6.2×10^2
0	7	n	1.9×10^{16}	6.6×10^3	90	p	4.9×10^{15}	6.0×10^2
0	15	n	1.8×10^{16}	6.8×10^3	90	p	6.1×10^{15}	6.7×10^2

TABLE II. Hall measurements at $B = 0.2$ T for 2-in.-diam $Hg_{1-x}Cd_xTe$ (100) film grown at 185 °C on CdTe (100)/GaAs (100) substrate. Sample No. 750576. $x = 0$, $y = 0$ is at the center of the sample.

x (mm)	y (mm)	Cond. type	300 K $N_d - N_a$ (cm^{-3})	300 K μ_H ($cm^2 V^{-1} s^{-1}$)	Cond. type	23 K $N_d - N_a$ (cm^{-3})	23 K μ_H ($cm^2 V^{-1} s^{-1}$)
0	0	n	3.6×10^{16}	1.2×10^4	n	4.2×10^{15}	1.3×10^5
11	0	n	4.0×10^{16}	1.0×10^4	n	4.0×10^{15}	1.3×10^5
11	3	n	4.5×10^{16}	1.1×10^4	n	4.2×10^{15}	1.5×10^5
0	6	n	3.9×10^{16}	1.1×10^4	n	4.2×10^{15}	1.4×10^5
0	9	n	4.0×10^{16}	9.8×10^3	n	4.2×10^{15}	1.3×10^5
0	13	n	6.2×10^{16}	9.2×10^3	n	4.4×10^{15}	1.3×10^5
0	20	n	6.3×10^{16}	1.1×10^4	n	4.3×10^{15}	1.8×10^5

almost achieved on 2-in.-diam $Hg_{1-x}Cd_xTe$ films. For the reported n-type film the uniformity of x was almost as good with $\Delta x/\bar{x} = 1.4\%$, as shown in Fig. 3. For this n-type film the thickness (e) was very uniform with $\Delta e/\bar{e} = 0.6\%$.

Each 2-in.-diam $Hg_{1-x}Cd_xTe$ film also showed complete uniformity over its surface in the conduction type exhibited. That is, p-type films were entirely p type, and n-type films were entirely n type. The carrier concentrations ($N_a - N_d$ or $N_d - N_a$) and the Hall mobilities (μ_H), however, showed some variation as may be seen in Tables I and II. It should be pointed out that both the electron and the hole mobilities are high for this cadmium concentration and attest to the high quality of the material grown here. The carrier concentrations are also in a range suitable for photovoltaic devices.

For both the p-type and n-type films reported here, nonuniformities in the carrier concentrations or the x values indicate variations in the sample temperature and Hg flux over the surface of the samples. Other hypotheses which have not been considered here, such as the role of the crystallographic orientation, could also contribute to the structural and electrical parameters observed. In order to grow $Hg_{1-x}Cd_xTe$ epilayers on even larger substrates, more uniform sample temperatures (which ideally must be constant within 1 °C) and a more uniform Hg flux are required.

In summary, it has been demonstrated here that high-quality $Hg_{1-x}Cd_xTe$ films of 2-in. diameter can be grown by MBE. High Hall mobilities, low carrier concentrations, uniform thicknesses, and very uniform Cd concentrations have been achieved already in these films which make them suitable for infrared device applications. These uniformities are much better than those currently achieved using the organometallic vapor phase epitaxy (OMVPE) growth method ($\Delta x = \pm 0.004$ for a 1-in. square CdTe substrate[9] and $\Delta x = \pm 0.005$ for a 1×2 cm^2 CdTeSe substrate[10]). This achievement represents a major step toward the future of infrared detector technology which demands ever greater uniformity over ever larger surface areas. We have demonstrated here that MBE is a prominent growth technique which can fulfill this requirement. Further improvements in the temperature uniformity of the sample, along with increased uniformity of the Hg flux on the sample, are expected to produce $Hg_{1-x}Cd_xTe$ films of even better uniformity on larger surface areas.

The authors would like to thank P. S. Wijewarnasuriya for performing the Hall measurements and the Defense Advanced Research Projects Agency for its financial support under contract F49620-87-C-0021, monitored by the Air Force Office for Scientific Research.

[1] S. C. Jackson, B. N. Baron, R. E. Rocheleau, and T. W. F. Russel, J. Vac. Sci. Technol. A 3, 1916 (1985).
[2] J. P. Faurie, J. Reno, S. Sivananthan, I. K. Sou, X. Chu, M. Boukerche, and P. S. Wijewarnasuriya, J. Vac. Sci. Technol. B 4, 585 (1986).
[3] S. Sivananthan, M. D. Lange, X. Chu, and J. P. Faurie, J. Vac. Sci. Technol. (to be published).
[4] R. F. C. Farrow, J. Vac. Sci. Technol. A 3, 60 (1985).
[5] N. Otsuka, L. A. Kolodziejski, R. L. Gunshor, S. Datta, R. W. Bicknell, and J. F. Schetzina, Proceedings of the Materials Research Society Meeting, Boston, Nov. 1984.
[6] J. P. Faurie, C. Hsu, S. Sivananthan, and X. Chu, Surf. Sci. 168, 473 (1986) and references therein.
[7] S. Sivananthan, X. Chu, J. Reno, and J. P. Faurie, J. Appl. Phys. 60, 1359 (1986).
[8] G. L. Hansen, J. L. Schmit, and T. N. Casselman, J. Appl. Phys. 53, 7099 (1982).
[9] S. J. C. Irvine, J. S. Gough, J. Giess, J. B. Mullin, and G. Crimes, 1987 U.S. Workshop on the Physics and Chemistry of HCT, Oct. 1987 (unpublished result).
[10] I. B. Bhat, H. Fardi, S. K. Ghandhi, and C. J. Johnson, 1987 U.S. Workshop on the Physics and Chemistry of Mercury Cadmium Telluride, New Orleans, Oct. 1987, Extended Abstracts, p. VII-9.

Electrical determination of the valence-band discontinuity in HgTe-CdTe heterojunctions

D. H. Chow, J. O. McCaldin, A. R. Bonnefoi, and T. C. McGill
T. J. Watson, Sr., Laboratory of Applied Physics, California Institute of Technology, Pasadena, California 91125

I. K. Sou and J. P. Faurie
Department of Physics, University of Illinois at Chicago, Chicago, Illinois 60680

(Received 17 August 1987; accepted for publication 22 October 1987)

Current-voltage behavior is studied experimentally in a $Hg_{0.78}Cd_{0.22}Te$-CdTe-$Hg_{0.78}Cd_{0.22}Te$ heterostructure grown by molecular beam epitaxy. At temperatures above 160 K, energy-band diagrams suggest that the dominant low-bias current is thermionic hole emission across the CdTe barrier layer. This interpretation yields a direct determination of 390 ± 75 meV for the HgTe-CdTe valence-band discontinuity at 300 K. Similar analyses of current-voltage data taken at 190–300 K suggest that the valence-band offset decreases at low temperatures in this heterojunction.

The HgTe-CdTe heterojunction is the building block for a number of interesting device structures which have been experimentally realized. These include the HgTe-CdTe superlattice,[1-7] the resonant tunneling HgTe-$Hg_{1-x}Cd_xTe$ double barrier heterostructure,[8,9] and the single barrier $Hg_{1-x}Cd_xTe$ negative differential resistance heterostructure.[10,11] In all of these structures, the valence-band offset, ΔE_v at the HgTe-CdTe interface is an important quantity in determining device behavior. Several theoretical and experimental values of ΔE_v have been reported.[12-20] Most recently, x-ray photoemission spectroscopy (XPS) experiments on HgTe-CdTe heterojunctions have yielded values of approximately 350 meV for ΔE_v at room temperature.[16-18] These results are in serious disagreement with most interpretations of published superlattice photoluminescence data, which indicate that ΔE_v must be nearly 0 meV to explain the observed high-energy luminescence.[3-7] The XPS results are also in apparent disagreement with earlier low-temperature magnetoabsorption experiments which yielded a value of 40 meV for ΔE_v,[20] although it has been suggested that these two measurements could be consistent with each other if ΔE_v is temperature dependent.[21]

In this letter, we report a direct electrical measurement of the valence-band discontinuity at the HgTe-CdTe interface. The sample studied was grown on a semi-insulating GaAs substrate by molecular beam epitaxy (MBE) in a Riber 2300 system. The active region consisted of a CdTe barrier layer sandwiched between two $Hg_{0.78}Cd_{0.22}Te$ electrodes. Transmission electron microscopy (TEM) showed that the CdTe layer was 180 Å thick. The $Hg_{0.78}Cd_{0.22}Te$ electrodes were doped n type with indium, to a carrier concentration of 3.6×10^{16} cm^{-3} at 30 K. The top (bottom) electrode was 0.5 μm (3 μm) thick. A 2.5-μm CdTe buffer layer preceded the growth of the active device region of the heterostructure. Mesas were fabricated in the sample by wet etching with Br_2:HBr:H_2O in a 0.005:1:3 ratio. Au was used to make ohmic contacts to both the tops of the mesas and the etched $Hg_{0.78}Cd_{0.22}Te$ surface, forming a set of isolated two-terminal devices. The mesas were circular, with diameters ranging from 35 to 70 μm. Several distinct preparations of the sample were performed, with over 100 devices tested in total at room temperature. Roughly 25% of the devices were "short-circuits," with markedly higher currents and nearly linear current-voltage (I-V) curves. The remainder of the devices displayed uniform behavior, with overall current densities deviating by no more than 20%. Measured currents from the fabricated devices were found to be proportional to device area, indicating that edge transport mechanisms were not significant.

Figure 1 is an energy-band diagram for the heterostructure under an applied bias of 50 mV, calculated by solving Poisson's equation self-consistently via the method of Bonnefoi *et al.*[22] It should be noted that the calculated band diagram is independent of the values of the band offsets, except for an overall shift of the conduction- and valence-band edges in the CdTe layer. Figure 1 suggests that the dominant source of current at high temperatures is the thermionic emission of holes from the $Hg_{0.78}Cd_{0.22}Te$ cladding layers across the CdTe valence-band barrier. It is important to note that the n-type doping of the electrodes does not

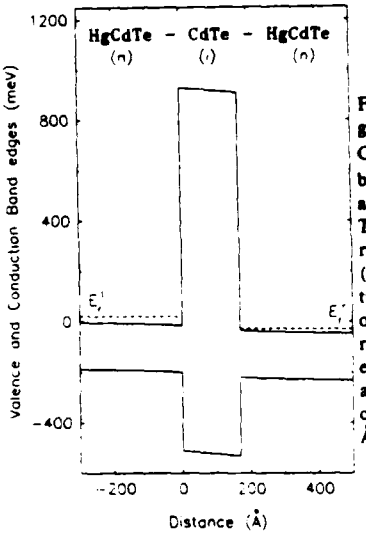

FIG. 1. Calculated band diagram for the $Hg_{0.78}Cd_{0.22}Te$-CdTe-$Hg_{0.78}Cd_{0.22}Te$ single barrier heterostructure, under an applied voltage of 50 mV. The upper (lower) solid line represents the conduction- (valence-) band edge as a function of distance in the direction of growth. The dashed line represents the Fermi energy in each of the electrodes, which are doped n type at 3.6×10^{16} cm^{-3}. The CdTe barrier is 180 Å thick.

 0003-6951/87/522230-03$01.00

prohibit this transport mechanism because the band gap in $Hg_{0.78}Cd_{0.22}Te$ is small ($\approx$200 meV).[23] At zero applied bias, the size of the potential energy barrier which the holes cross is given by

$$\phi_{\text{hole}} = E_f + E_g^{(x=0.22)} + \Delta E_v^{(x=0.22)},$$

where E_f is the Fermi energy relative to the conduction-band edge in the $Hg_{0.78}Cd_{0.22}Te$ electrodes, $E_g^{(x=0.22)}$ is the electrode band gap, and $\Delta E_v^{(x=0.22)}$ is the valence-band offset between $Hg_{0.78}Cd_{0.22}Te$ and CdTe. For all reported theoretical and experimental values of ΔE_v, the potential energy barrier for thermionic emission of electrons is much larger than ϕ_{hole}. It follows that thermionic electron currents can be ignored for this heterostructure.

A simple theoretical treatment, similar to the Bethe model for Schottky barriers,[24] can be employed to calculate thermionic hole current densities across the CdTe barrier as a function of applied voltage. The resulting expression is

$$J_{\text{therm}} = A^* T^2 \exp\left(\frac{-\phi_{\text{hole}} + cqV}{kT}\right)\left[1 - \exp\left(\frac{-qV}{kT}\right)\right],$$

where A^* is the modified Richardson constant, T is the temperature, V is the applied voltage, q is the hole charge, k is the Boltzmann constant, and c is the fraction of the total applied voltage which drops across the positively biased $Hg_{0.78}Cd_{0.22}Te$ electrode. For this single barrier heterostructure, A^* is $120(m_h^*)$ in A/cm^2 K^2, where m_h^* is the unitless hole mass. The contributions from the light- and heavy-hole bands are summed to give the total current from this mechanism. It is important to note that the factor c is a function of the voltage applied across the heterostructure, and must therefore be calculated from the energy-band diagram for each individual bias condition. The value of c generally is in the range 0.25–0.40 for the heterostructure studied here, as compared to the case of a Schottky barrier, where $c = 1$.

For applied voltages of approximately 50 mV and higher, tunneling of holes across the "triangular-shaped" CdTe barrier makes a contribution to the total current through the heterostructure. This transport mechanism can be treated theoretically in a manner which is analogous to the model for the thermionic hole current. The resulting expression for the hole tunneling current density, J_{htun}, differs from that for J_{therm} by an integral term which replaces the factor $\exp(-\Delta E_v^{(x=0.22)}/kT)$:

$$J_{\text{htun}} = A^* T^2 \exp\left(\frac{-E_f - E_g^{(x=0.22)} + cqV}{kT}\right) \times \left[1 - \exp\left(\frac{-qV}{kT}\right)\right]\int_0^{u_0} (t^* t)\, u \exp\left(\frac{-u^2}{2}\right) du .$$

In this expression,

$$u^2/2 = m_h^* v_l^2/kT,$$

where v_l is the group velocity of the holes in the growth direction, $u_0 = (2\Delta E_v^{(x=0.22)}/kT)^{1/2}$, and t^*t is the transmission coefficient for holes tunneling through the CdTe barrier. In this study, we have calculated t^*t via the Wentzel–Kramers–Brillouin (WKB) method. A two-band $k\cdot p$ theory formula[25] was used to find imaginary light-hole wave vectors in the CdTe barrier, while imaginary heavy-hole wave vectors were determined from the simple "one-band" formula.

The total current density J is the sum of J_{therm} and J_{htun}. In general, the thermionic current density is calculated more accurately than the tunneling current density because t^*t is strongly dependent on many parameters, such as the barrier thickness, CdTe effective masses, and the applied voltage. It is therefore prudent to restrict analysis of experimental data to those voltages at which J_{therm} is expected to dominate. For this heterostructure, it has been estimated that J_{htun} becomes large (greater than 30% of the current) when $V > 100$ mV. At room temperature, J_{therm} and J_{htun} are much greater than the electron tunneling current J_{etun}. However, negative differential resistance regions have been observed in I-V characteristics taken at $T = 4.2$ K, indicating that electron tunneling becomes an important transport mechanism at low temperatures. These results will be reported elsewhere.[11]

Figure 2 contains a typical experimental current density-voltage (J-V) characteristic, taken at room temperature. Also shown is a theoretical curve, which is obtained by setting $\Delta E_v^{(x=0.22)} = 285$ meV in our simple model of the J-V behavior. $\Delta E_v^{(x=0.22)}$ was chosen by requiring the calculated and experimental currents to be the same at 50 mV, and was the only adjustable parameter used. Selecting different values of the applied bias results in variations of $\Delta E_v^{(x=0.22)}$ by roughly $\pm$ 10 meV over the voltage range 0–200 mV, well beyond the 100-mV limit discussed above. This supports the assertion that virtually all of the current in the heterostructure is due to J_{therm} and J_{htun}. In fact, the shape of the theoretical J-V curve is nearly independent of the choice of $\Delta E_v^{(x=0.22)}$, which enters the expression for J_{therm} only in a voltage-independent multiplicative factor. Over 75 devices (those which were not shorted, as described previously) were tested at room temperature. In all cases, $\Delta E_v^{(x=0.22)}$ was found to be within 10 meV of the value obtained in Fig. 2. Due to the presence of Hg flux during the growth of CdTe layers, it is expected that the barrier material is actually $Hg_{0.05}Cd_{0.95}Te$.[26] Therefore, the experimentally obtained value of $\Delta E_v^{(x=0.22)}$ actually represents the valence-band discontinuity at a $Hg_{0.78}Cd_{0.22}Te$-$Hg_{0.05}Cd_{0.95}Te$ interface.

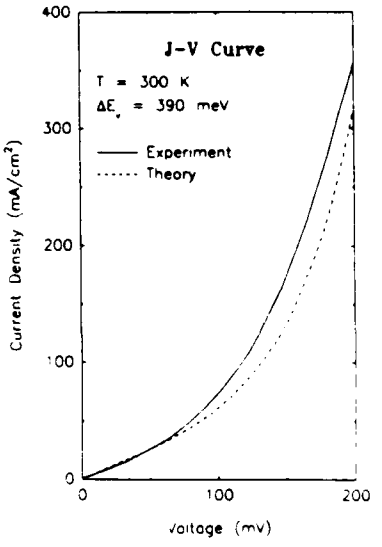

FIG. 2. Experimental J-V curve (solid line) taken at room temperature. Also plotted is a best fit curve calculated for a HgTe-CdTe valence-band offset of 390 meV (dashed line). ΔE_v is the only adjustable parameter used to generate the best fit curve.

Assuming a linear variation of the valence-band edge in $Hg_{1-x}Cd_xTe$ with x, ΔE_v is then determined to be 390 ± 75 meV. The estimated error has been assigned by combining the previously discussed variation in $\Delta E_v^{(x=0.22)}$ with the following sources of uncertainty: (i) nonuniformity across the sample, (ii) uncertainty in cladding layer compositions and band gaps, (iii) the percentage of alloying of the CdTe barrier due to incorporation of Hg during growth, and (iv) errors made in determining the transmission coefficients for hole tunneling.

Further I-V measurements were made on over 20 devices in a low-temperature microprobe station. Electron tunneling currents were found to be insignificant for temperatures above 160 K. Consequently, we report data here for 190 K and higher. Analysis of the low-temperature data was performed in the same manner as described previously for room-temperature measurements, producing theoretical J-V curves which agreed within 5% of the experimental characteristics over the voltage range 0–100 meV.

Figure 3 is a plot of the values of ΔE_v which were determined as a function of temperature, along with a corresponding scale for $\Delta E_v^{(x=0.22)}$. Examination of Fig. 3 reveals that the band offset is found to vary strongly with temperature—an effect that has not been reported previously, to the best of the authors' knowledge. For example, it is found that $\Delta E_v = 245 \pm 70$ meV at $T = 190$ K. Band offset theories are at an early stage of development, with no temperature dependence yet estimated. It is possible that a transport mechanism which has not been considered may be contributing to the observed currents. This could lead to false determinations of the low-temperature band offsets. However, the observed agreement between the theoretical and experimental J-V curves, without the use of any free parameters other than $\Delta E_v^{(x=0.22)}$, suggests that the correct current transport mechanisms have been included. It should be noted that the observed current decreases exponentially as the temperature decreases (as is expected for thermionic mechanisms), despite the decrease in ΔE_v. This is reasonable because ϕ_{hole} includes terms which do not vanish at $T = 0$ K. Furthermore, the recent observation of negative differential resistance at $T = 4.2$ K is consistent with a valence-band offset

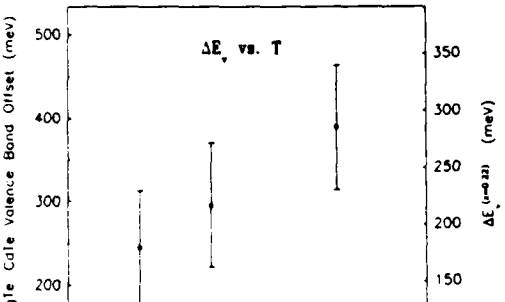

FIG. 3. Temperature dependence of HgTe-CdTe valence-band offset, as determined from experimental J-V curves. Also plotted is the corresponding scale for the offset at the $Hg_{0.78}Cd_{0.22}Te$-$Hg_{0.05}Cd_{0.95}Te$ interface, $\Delta E_v^{(x=0.22)}$, assuming a linear dependence on composition, i.e., $\Delta E_v^{(x=0.22)} = 0.73\Delta E_v$.

which is much smaller than the room-temperature value.[11]

In this letter, we have experimentally and theoretically studied the current-voltage behavior of a $Hg_{0.78}Cd_{0.22}Te$-CdTe-$Hg_{0.78}Cd_{0.22}Te$ heterostructure. Interpretation of the measured current as being dominated by thermionic and tunneling hole currents resulted in a determination of $\Delta E_v = 390 \pm 75$ meV at $T = 300$ K. This result is in reasonable agreement with recent XPS measurements. A similar analysis of low-temperature data indicates that the valence-band offset has a strong and previously unreported temperature dependence, with ΔE_v becoming smaller for low T. However, other transport mechanisms may have contributed to the low-temperature currents, leading to erroneously low values of ΔE_v.

We wish to acknowledge S. Nieh for providing us with important TEM data, and O. J. Marsh, T. K. Woodward, and M. B. Johnson for valuable discussions and assistance. This work was supported by the Defense Advanced Research Projects Agency under contract No. N00014-86-K-0841 and No. F49620-87-C-0021. One of us (DHC) received financial support from International Business Machines Corporation.

[1] J. N. Schulman and T. C. McGill, Appl. Phys. Lett. 34, 663 (1979).
[2] C. E. Jones, T. N. Casselman, J. P. Faurie, S. Perkowitz, and J. N. Schulman, Appl. Phys. Lett. 47, 140 (1985).
[3] S. R. Hetzler, J. P. Baukus, A. T. Hunter, J. P. Faurie, P. P. Chow, and T. C. McGill, Appl. Phys. Lett. 47, 260 (1985).
[4] J. P. Faurie, J. Reno, and M. Boukerche, J. Cryst. Growth 72, 111 (1985).
[5] J. P. Baukus, A. T. Hunter, O. J. Marsh, C. E. Jones, G. Y. Wu, S. R. Hetzler, T. C. McGill, and J. P. Faurie, J. Vac. Sci. Technol. A 4, 2110 (1986).
[6] D. J. Leopold, M. L. Wroge, and J. G. Broerman, Appl. Phys. Lett. 50, 924 (1987).
[7] J. P. Baukus, A. T. Hunter, J. N. Schulman, and J. P. Faurie (unpublished).
[8] J. N. Schulman and C. L. Anderson, Appl. Phys. Lett. 48, 1684 (1986).
[9] M. A. Reed, R. J. Koestner, and M. W. Goodwin, Appl. Phys. Lett. 49, 1293 (1986).
[10] D. H. Chow and T. C. McGill, Appl. Phys. Lett. 48, 1485 (1986).
[11] D. H. Chow, T. C. McGill, I. K. Sou, J. P. Faurie, and C. W. Nieh (unpublished).
[12] J. O. McCaldin, T. C. McGill, and C. A. Mead, Phys. Rev. Lett. 36, 56 (1976).
[13] W. A. Harrison, *Electronic Structure and The Properties of Solids* (Freeman, San Francisco, 1980).
[14] J. Tersoff, J. Vac. Sci. Technol. B 4, 1066 (1986).
[15] T. F. Kuech and J. O. McCaldin, J. Appl. Phys. 53, 3121 (1982).
[16] S. P. Kowalczyk, J. T. Cheung, E. A. Kraut, and R. W. Grant, Phys. Rev. Lett. 56, 1605 (1986).
[17] T. M. Duc, C. Hsu, and J. P. Faurie, Phys. Rev. Lett. 58, 1127 (1987).
[18] C. K. Shih and W. E. Spicer, Phys. Rev. Lett. 58, 2594 (1987).
[19] A. Zoryk and M. Jaros, Appl. Phys. Lett. 50, 1191 (1987).
[20] Y. Guldner, G. Bastard, J. P. Vieren, M. Voos, J. P. Faurie, and A. Million, Phys. Rev. Lett. 51, 907 (1983).
[21] J. P. Faurie, C. Hsu, and T. M. Duc, J. Vac. Sci. Technol. A 5, 3074 (1987).
[22] A. R. Bonnefoi, D. H. Chow, and T. C. McGill, to be published in J. Appl. Phys.
[23] R. Dornhaus, G. Nimtz, and B. Schlicht, *Narrow-Gap Semiconductors* (Springer, Berlin, 1983), pp. 158–160.
[24] S. M. Sze, *Physics of Semiconductor Devices* (Wiley, New York, 1981), pp. 255–259.
[25] E. O. Kane, *Physics of III-V Compou...* (Academic, New York, 1966), Vol. 1, Chap. 3, pp. 75–100.
[26] J. Reno, R. Sporken, Y. J. Kim, C. Hsu, and J. P. Faurie (unpublished).

PHYSICAL REVIEW B VOLUME 38, NUMBER 0 15 JULY 1988

X-ray photoemission from small mercury clusters on II-VI semiconductor surfaces

R. Sporken,* S. Sivananthan, J. Reno,† and J. P. Faurie
Department of Physics, University of Illinois at Chicago, P.O. Box 4348, Chicago, Illinois 60680
(Received 16 October 1987)

The presence of small Hg clusters ($R \approx 5$–20 Å) on $Hg_{1-x}Cd_xTe$ samples grown by molecular-beam epitaxy has been deduced from a careful analysis of the x-ray-induced photoemission spectra. The positive binding-energy shift measured for these clusters is explained by the appearance of a positive charge on the clusters during the photoemission process. (The experimental results are compared with the calculated $e^2/2R$ behavior.) The apparent spin-orbit splitting for the Hg $5d$ levels is reduced, compared to bulk Hg and to isolated Hg atoms. This is attributed to the repulsion between the Cd $4d$ and Hg $5d$ orbitals. It is shown that Hg out-diffusion is the main reason for the formation of these clusters.

MS code no. BKR398B 1988 PACS number(s): 79.60.—i

I. INTRODUCTION

Studies of surfaces and interfaces of semiconducting materials are very important for the development and understanding of modern microelectronic devices. Detailed investigation of the phenomena occurring during the growth of such surfaces and interfaces is very important due to the still increasing miniaturization of the devices presenting a challenge to both theoreticians and experimentalists. This paper deals with one particular aspect of surface studies on II-VI compound semiconductors, which is the formation of small mercury clusters on the surfaces of these semiconductors.

Photoemission has been demonstrated to be very powerful for examining the electronic properties of supported small metal clusters.[1–3] The study of such small particles was initially motivated by their technological importance in heterogeneous catalysis.[4] Small metal clusters have also been detected in many cases during the early stages of metal-semiconductor interface formation.[5–7] Amorphous carbon has been the most widely used substrate for detailed studies of the electronic properties of small metal clusters, but other substrates, mostly insulators, have been used as well. In this paper we present a photoemission study of Hg clusters on CdTe(111) and $Hg_{1-x}Cd_xTe$(111) substrates. To the best of our knowledge, this is the first detailed photoemission study of metal clusters on a semiconducting substrate.

This work was first motivated by an unexpected result obtained during the study of the Hg incorporation in CdTe during the growth of HgTe-CdTe superlattices by molecular-beam epitaxy (MBE).[8] The common growth technique for HgTe-CdTe superlattices and other superstructures, such as single and double barrier tunneling structures, involves leaving the Hg cell open at all times.[9,10] As a result, the CdTe layers are not pure CdTe layers, but instead $Hg_{1-x}Cd_xTe$ with typically 3–9 % of mercury for the (111) B orientation.[8] In addition to Hg bound to Te atoms, the x-ray photoemission (XPS) analysis of such spectra revealed the existence of a second type of mercury with about 600 meV higher binding energy.[8] In the present work, we show that this second mercury component in the Hg $5d$ and $4f$ spectra is due to the presence of small Hg clusters on CdTe and $Hg_{1-x}Cd_xTe$ surfaces. The electronic properties as well as the origin of these clusters will be discussed.

II. EXPERIMENTAL

The samples were all prepared at the University of Illinois at Chicago in a Riber MBE 2300 machine. CdTe substrates oriented in the (111) B direction as well as GaAs substrates with a CdTe(111) B buffer layer were used. The substrate preparation and the growth of the appropriate buffer layer have been discussed elsewhere.[9] The layers analyzed here are $Hg_{1-x}Cd_xTe$ with x in the range of 0.15–0.97. The smaller x values were obtained with three MBE sources (CdTe, Te, and Hg) following the usual procedure.[9] The larger values are obtained with only two sources (CdTe and Hg) as described in Ref. 8. The sample temperatures quoted here were measured using a Chromel-Alumel thermocouple and—whenever possible—by an infrared pyrometer. These measurements have been calibrated using the melting points of indium and tin.

The samples were kept under ultrahigh-vacuum conditions as they were transferred to the XPS chamber. The XPS measurements were performed with a SSX-100 spectrometer from Surface Science Laboratories. A monochromatized and focussed Al $K\alpha$ excitation line was used. The overall energy resolution measured on the Au $4f$ core level is 0.7 eV. The reference levels used for this study will be specified as necessary. The position of the Fermi level was determined from the position of the Au $4f_{7/2}$ line measured from a bulk gold sample. The corresponding binding energy was fixed at 83.93 eV. The core levels used in this work are the Hg $4f$ and $5d$, the Cd $3d$ and $4d$, and the Te $4d$ and $3d$. For all the peaks, the values of the area, position, and full width at half maximum (FWHM) were determined by a least-squares fit of individual spin-orbit doublets to the data.

III. RESULTS AND DISCUSSION

The discussion of the results will be organized in three parts. First, we will focus on a detailed analysis of the XPS spectra from $Hg_{1-x}Cd_xTe$ samples. It will be shown that two types of Hg exist in these samples, one being Hg bound to Te and the other due to the presence of small mercury clusters on the sample surface. Hereafter, it will be shown that such Hg clusters can be obtained by depositing Hg on CdTe(111) *B* surfaces at room temperature. Finally, we will try to identify the origin of these clusters obtained unintentionally on MBE-grown $Hg_{1-x}Cd_xTe$ surfaces.

Typical photoemission spectra from $Hg_{1-x}Cd_xTe$ are shown in Fig. 1. The peaks are the Cd 4*d* and Hg 5*d* spin-orbit doublets and the Hg $4f_{7/2}$. These spectra have been analyzed for all the samples by means of a least-squares curve-fitting procedure as mentioned above. A nonlinear background was subtracted from the spectra prior to the fitting procedure. The line shape used for the fits was a Lorentzian convoluted with a Gaussian. This procedure is justified for the photoemission from semiconductors. It might be argued, however, that the Doniach-Šunjić line shape[11] has to be used in the case of small metal clusters. The quality of the fits obtained with the symmetric line shape is very good. This might indicate that the final-state screening in very small clusters is different from bulk metals, resulting in a different (and smaller) singularly index for the Doniach-Šunjić line shape for these clusters as compared to the bulk metal.

Two types of Hg have consistently been found for all the samples. These two types of mercury will be labeled $Hg^{(1)}$ and $Hg^{(2)}$ in the following discussion. From its binding energy with respect to the valence-band maximum (VBM),[12] $Hg^{(1)}$ is clearly identified as Hg in $Hg_{1-x}Cd_xTe$. The second component $Hg^{(2)}$ is observed at higher binding energy. We have suggested earlier that $Hg^{(2)}$ is due to some kind of surface mercury.[8] This was inferred from two observations. First, on a 1.5-μm-thick CdTe layer grown with a Hg flux, the amount of incorporated Hg as measured with energy-dispersive x-ray spectroscopy (EDS) agrees with the results from XPS obtained by neglecting $Hg^{(2)}$. Including $Hg^{(2)}$ yields significantly higher concentrations. As the depth probed by XPS is small compared to EDS, $Hg^{(2)}$ should be located in the surface region. Second, the Hg concentration in the CdTe layers can be determined from the binding energy of the Cd 4*d* and Hg 5*d* levels with respect to the VBM. This procedure is described in Ref. 8. Once again these results agree with concentrations deduced from XPS peak areas, neglecting $Hg^{(2)}$. This also suggests that $Hg^{(2)}$ is located at the surface. Otherwise it would affect the position of the VBM.

Now that we have established that $Hg^{(2)}$ is some sort of surface mercury, we need to find its exact nature. From the chemical shift measured on the Hg 5*d* and Hg 4*f* lines, $Hg^{(2)}$ could be tentatively identified as $HgTe_2$. This is not a stable compound, but could exist at the surface of $Hg_{2-x}Cd_xTe$ samples. However, if $Hg^{(2)}$ is located in a two-dimensional surface layer, coverages up to 0.8 monolayers (ML) are deduced from the $Hg^{(2)}$ peak areas. Such a coverage should then affect the characteristics of a surface component detected in the Te 4*d* spectra. The surfaces studied here are (111) *B* surfaces which are ter-

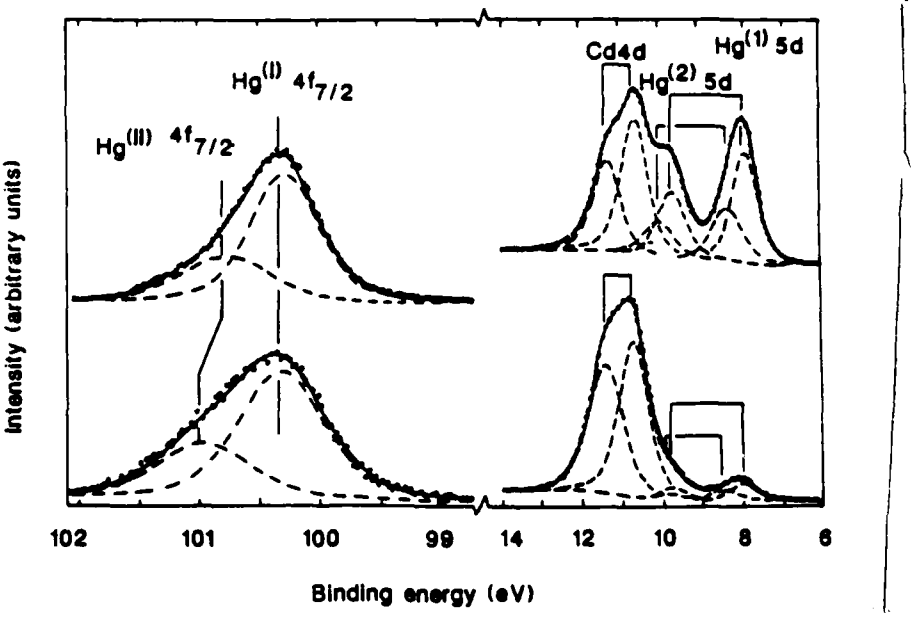

FIG. 1. Typical XPS core-level spectra from $Hg_{1-x}Cd_xTe$. The composition is $x=0.94$ (lower spectrum) and $x=0.60$ (upper spectrum). The number of atoms in the $Hg^{(2)}$ estimated using relation (1) is 7×10^{13} and 6×10^{14} cm^{-2}, respectively. The binding energy is referred to the Fermi level. The solid line is obtained by least-squares fitting of individual components (dashed lines) to the data.

minated by threefold-bonded Te atoms. From the Te 4*d* core-level spectra, a surface shift[13] of 475±75 meV towards higher binding energy was unambiguously determined by very careful curve fitting (Fig. 2). Close examination of the residuals, i.e., the difference between the calculated and the measured spectra, was particularly useful for the determination of this surface component. The characteristics (relative intensity, FWHM, and shift) of this surface component are independent of the amount of $Hg^{(2)}$. This rules out the existence of a two-dimensional layer of $HgTe_2$.

Based on this observation and on the fact that the Te 4*d* core-level intensity is reduced by only 5% for a $Hg^{(2)}$ coverage corresponding to 1 ML in the case of a two-dimensional layer, we suggest that $Hg^{(2)}$ must be related to the existence of small Hg clusters on the sample surface. The spectral characteristics of such small metal clusters are now well established[1-3,14,15] although the detailed explanation of these same characteristics is still a matter of debate. For almost all cases of small metal clusters, the core-level binding energies are higher than for the corresponding bulk material. This binding energy generally decreases with increasing cluster size, and sometimes a saturation or even a slight decrease is observed for very small cluster sizes.[3,14]

Figure 3 shows the binding energy E_B with respect to the Fermi level for the $Hg^{(2)}$ $4f_{7/2}$ core level versus the $A(Hg^{(2)}\,4f_{7/2})/A(Te\,3d_{5/2})$ area ratio. These data have been measured from many different samples and the different area ratios are the results of different preparation conditions. The relation between this area ratio and the preparation conditions will be discussed in the last section of this paper. The $A(Hg)/A(Te)$ area ratio is related to the average cluster radius. The intensity model described in Ref. 14 can be adapted to the present problem and the following relation is obtained:

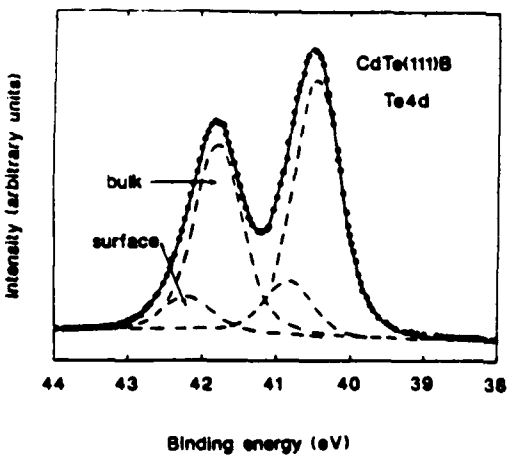

FIG. 2. Te 4*d* core-level spectrum from CdTe(111) *B*. The solid line is obtained by least-squares fitting of individual components (dashed lines) to the data. The binding-energy scale is referred to the Fermi level.

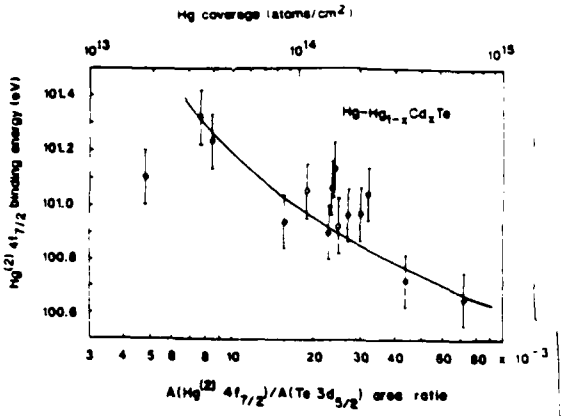

FIG. 3. $Hg^{(2)}$ $4f_{7/2}$ binding energy with respect to the Fermi level, vs $A(Hg^{(2)}\,4f_{7/2})/A(Te\,3d_{5/2})$ area ratio. The solid circles are results from $Hg_{1-x}Cd_xTe$ samples, whereas the open circles are obtained after the Hg absorption on CdTe at room temperature. The Hg coverage has been estimated using relation (1) with $N_c = 6\times10^{11}$ cm^{-2}. The solid line represents the calculated $e^2/2R$ behavior. For details see the text.

$$\Gamma = A(Hg^{(2)}\,4f_{7/2})/A(Te\,3d_{5/2})$$
$$= N_c k \lambda_e \{R^2 - 2[\lambda_e^2 - (R\lambda_e + \lambda_e^2)\exp(-R/\lambda_e)]\} . \quad (1)$$

This relation is valid as long as the area covered by the clusters is small compared to the total sample area. R is the average cluster radius, N_c the cluster concentration, λ_e the effective photoelectron escape depth, and k is a constant depending on XPS sensitivity factors and on the density of the Hg clusters. λ_e is related to the photoelectron escape depth λ and to the mean electron escape angle β ($\lambda_e = \lambda\cos\beta$). If N_c has approximately the same value for all the samples studied here, a plot of E_B versus Γ is equivalent to a plot of E_B versus R on a nonlinear scale. Some scatter observed from our data is most likely due to slight differences in N_c between different samples. The binding-energy decrease observed in Fig. 3 with increasing cluster size is a common feature for small metal clusters. In the case of metal clusters supported on insulating substrates, Wertheim *et al.*[3,15] have shown that positive binding-energy shifts with decreasing cluster size can be attributed to the Coulomb energy $\sim e^2/2R$ which is due to the positive charge appearing on the cluster surface during the photoemission process. The unit charge in the photoemission final state is not neutralized during the time scale relevant to photoemission. The resulting Coulomb attraction will therefore increase the measured binding energy of the photoelectrons from the cluster. The same explanation was used in Ref. 14 for the case of Al clusters on Sb(111) substrates. We now suggest that this explanation may also be extended to the case of small metal clusters on certain semiconducting surfaces. For a typical cluster concentration of $N_c = 6\times10^{11}$ cm^{-2}, the cluster radii corresponding to Fig. 3 are found in the range of 5–20 Å using Eq. (1). A rough estimation of the

corresponding $Hg^{(2)}$ coverages Θ yields 10^{13}–10^{15} atoms/cm^2. These coverage values are rather insensitive to the values of N_c, whereas the quoted radii are more strongly dependent on N_c. The reasonably smooth behavior of the data in Fig. 3 over a narrow range for the cluster radii (5–20 Å) is an indirect evidence for N_c being relatively independent on the details of the sample preparation. Figure 3 compares very well with results published in the recent literature concerning Au on amorphous carbon[2,3] and Ag on amorphous carbon.[13] In all the cases, the binding energy for the bulk metal was obtained for coverages between 10^{15} and 10^{16} atoms/cm^2. Extrapolation of our results, according to a $e^2/2R$ dependence, yields $E_B(Hg^{(2)}\ 4f_{7/2}) = 100.2 \pm 0.2$ eV for large cluster sizes. This is close to the value for bulk Hg (99.9 eV).[16] The solid line in Fig. 3 shows this $e^2/2R$ behavior adjusted to our data, using the values for R deduced from Eq. (1) with $N_c = 6 \times 10^{11}$ cm^{-2}. There might be a saturation or even a slight decrease for very small cluster sizes, as already reported for Al on Sb(111).[14] However, we do not want to draw this conclusion, due to the insufficient number of data in this particular region.

Another striking feature of $Hg^{(2)}$ is the variation of the apparent spin-orbit splitting of the $Hg^{(2)}$ 5*d* levels with $Hg^{(2)}$ coverage Θ. Figure 4 shows this energy separation versus the intensity ratio Γ defined above. A total increase of 0.5 eV is observed with increasing cluster size. A saturation occurs at 1.7 eV, which is close to the value for bulk Hg (1.86 eV).[17] The spin-orbit splitting for isolated Hg atoms is known to be equal to the value for liquid Hg.[17] Our measured values of the apparent spin-orbit splitting are thus even smaller than the value for isolated atoms. This can be explained by the repulsion between the Cd 4*d* and Hg 5*d* levels, as initially discussed by Moruzzi *et al.*[18] In systems with two *d* metals, even

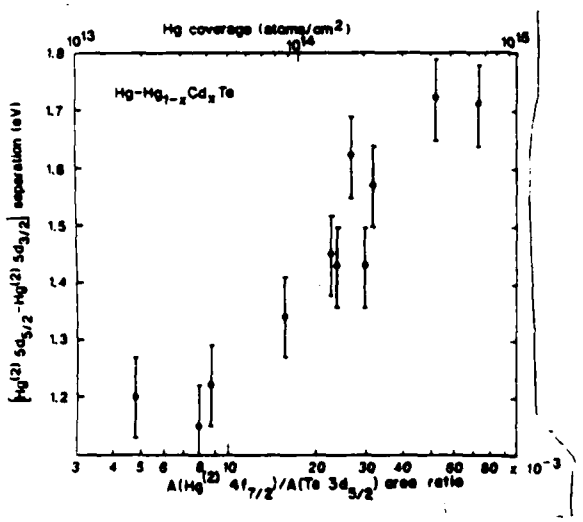

FIG. 4. $Hg^{(2)}$ 5*d* apparent spin-orbit splitting vs $A(Hg^{(2)}\ 5f_{7/2})/A(\text{Te}\ 3d_{5/2})$ area ratio. The Hg coverage has been estimated using relation (1) with $N_c = 10^{11}$ cm^{-2}. For details see the text.

with no direct energy overlap, the two sets of *d* levels interact. The result is a repulsion between these *d* states proportional to their original energy separation, which then reduces the apparent spin-orbit splitting of either subsystem. For the smallest clusters, almost all the $Hg^{(2)}$ atoms are in contact with the $Hg_{1-x}Cd_xTe$ surface, whereas the repulsion is reduced for the larger clusters due to the increased Cd—$Hg^{(2)}$ distance. A similar explanation has been invoked by Eberhardt *et al.* in the case of Cu_3Au alloys.[19]

We have adsorbed Hg on MBE-grown CdTe(111) samples. The samples were kept at room temperature and the estimated Hg flux was approximately 2.5×10^{17} atoms cm^{-2}s^{-1}. This value was determined using Knudsen's effusion law. Hg 4*f*, Cd 3*d*, and Te 3*d* spectra have been measured after exposures of 35 and 45 min, respectively. Only one component was then detected in the Hg $4f_{7/2}$ spectra. The corresponding results are represented by the open circles in Fig. 3. These results agree with values measured for $Hg^{(2)}$ on $Hg_{1-x}Cd_xTe$. This is a further evidence that our interpretation of $Hg^{(2)}$ is correct. We also note that for these two exposures, the ratio of the Hg coverages quoted in Fig. 3 is in excellent agreement with the ratio of the Hg exposures.

The last section of this paper is devoted to a tentative identification of the origin of the Hg clusters on $Hg_{1-x}Cd_xTe$ surfaces. Two possible sources of these Hg clusters are readily identified: either the Hg in the $Hg_{1-x}Cd_xTe$ crystals or the residual Hg in the growth chamber during the cooling of the grown layers.

The cooling of the layers from the growth temperature (175–195 °C) to a temperature low enough to take the samples out of the growth chamber (typically 50 °C) takes on the order of 1 h. During this time, the Hg flux is progressively reduced from a value of typically 1.5×10^{17} atoms cm^{-2}s^{-1} to zero. The amount of Hg in the clusters obtained by this procedure is comparable with the amount obtained by exposing a CdTe(111) *B* surface at room temperature to an estimated Hg flux of 2.5×10^{17} atoms cm^{-2}s^{-1} during at least 30 min. As the Hg sticking coefficient on CdTe is expected to decrease with increasing temperature and based on the fact that the Hg flux used for the adsorption experiment was always higher than during the cooling of the $Hg_{1-x}Cd_xTe$ samples, we conclude that Hg adsorption on the $Hg_{1-x}Cd_xTe$ surfaces during the cooling cannot be the only reason for the formation of Hg clusters on these surfaces. We therefore suggest that out-diffusion of Hg from the samples contributes significantly to the formation of the Hg clusters.

A mercury atom reaching the surface of a $Hg_{1-x}Cd_xTe$ sample can (1) combine with any available free Te atom, (2) migrate on the surface until it reaches a nucleation site and contribute to the formation of Hg clusters, or (3) desorb from the surface. Parameters like the substrate temperature or the number and type of surface defects certainly play a major role in determining which of these steps will be the dominant one. The three possibilities exist regardless of whether the Hg atom reaches the surface by out-diffusion from the bulk or by condensation from the Hg vapor. However, it is clear

that the amount of Hg in the sample should affect the amount of Hg in the clusters if out-diffusion is the major source of Hg atoms going into the clusters. Such a relation has been observed (Table I). For different samples prepared at the same temperature, the amount of Hg in the clusters is found to increase with the Hg concentration in the $Hg_{1-x}Cd_xTe$ samples. The exact relationship between the two intensities certainly depends on the distribution of the Hg in the clusters and in the $Hg_{1-x}Cd_xTe$, as well as on the details of the diffusion mechanism. Furthermore, the data in Table I are consistent with the assumption that the amount of Hg in the clusters increases with increasing temperature for a given sample composition. This would not be easy to explain if condensation from Hg vapor was the main reason for the cluster formation, whereas enhanced out-diffusion combined with higher surface mobility is likely to increase the amount of Hg in the clusters. However, increasing the substrate temperature also favors the Hg desorption. Many more experimental results as well as a detailed study of the corresponding surface kinetics are thus called for. A future study should also reveal whether the out-diffusing Hg was initially bound to Te or instead located in interstitial lattice sites. This is very important for an understanding of the thermal stability of these materials. The existence of interstitial Hg is indeed expected due to the high Hg overpressure needed during the growth of $Hg_{1-x}Cd_xTe$.[20]

TABLE I. Intensity ratio $A(Hg^{(2)}\ 4f_{7/2})/A(Te\ 3d_{5/2})$ for the Hg clusters along with the growth temperature and the composition of the $Hg_{1-x}Cd_xTe$ samples.

T_s (°C)	$1-x$	$A(Hg^{(2)}\ 4f_{7/2})/A(Te\ 3d_{5/2})$
185	0.065	9.7×10^{-3}
185	0.740	4.4×10^{-2}
195	0.045	4.8×10^{-3}
195	0.057	9.3×10^{-3}
195	0.085	1.6×10^{-2}
175	0.095	7.7×10^{-3}
185	0.065	9.7×10^{-3}
195	0.057	9.3×10^{-3}

IV. CONCLUSION

We have shown that Hg clusters are found on MBE-grown $Hg_{1-x}Cd_xTe$ samples. The typical radius of these clusters is in the range of 5–20 Å. The Hg core levels measured with XPS show the typical positive binding-energy shift which increases with decreasing cluster size. This shift is explained by the Coulomb energy $e^2/2R$ due to the positive charge appearing on the cluster during the photoemission process. For small clusters, the apparent spin-orbit splitting of the Hg $5d$ levels is smaller than for bulk Hg and even smaller than for isolated Hg atoms. This is attributed to repulsion between the Cd $4d$ and Hg $5d$ orbitals for the smallest clusters, where almost all the Hg atoms are in contact with the $Hg_{1-x}Cd_xTe$ substrate. Finally, we have shown that Hg out-diffusion from the bulk is probably the major reason for the formation of these clusters.

ACKNOWLEDGMENTS

We are grateful to Y. J. Kim for the preparation of some of the samples used for this work. This work carried out at the University of Illinois at Chicago, was supported by the U. S. Defense Advanced Research projects Agency and monitored by the U. S. Air Force Office of Scientific Research under Contract No. F4920-87-C-0021. One of us (R.S.) is supported in part by the Belgian National Foundation for Scientific Research [Fonds National Belge pom la Recherche Scientifique (FNRS)].

*Permanent address: Facultés Universitaires Notre-Dame de la Paix, B-5000 Namur, Belgium.
†Present address: Sandia National Laboratories, Organization 1144, Albuquerque, NM 87185-5800.

[1]K. S. Liang, W. R. Salaneck, and I. A. Aksay, Solid State Commun. 19, 329 (1976).
[2]M. G. Mason, Phys. Rev. B 27, 748 (1983).
[3]G. K. Wertheim, S. B. DiCenzo, and S. E. Younquist, Phys. Rev. Lett. 51, 2310 (1983).
[4]J. C. Slater and K. H. Johnson, Phys. Today 27, 34 (1974).
[5]T. Kendelewicz, W. G. Petro, I. Lindau, and W. E. Spicer, Phys. Rev. B 30, 5800 (1984).
[6]F. Houzay, M. Bensoussan, C. Guille, and F. Barthe, Surf. Sci. 162, 617 (1985).
[7]R. Sporken, P. Xhonneux, R. Caudano, and J. P. Delrue, Surf. Sci. (to be published).
[8]J. Reno, R. Sporken, Y. J. Kim, C. Hsu, and J. P. Faurie, Appl. Phys. Lett. 51, 1545 (1987).
[9]J. P. Faurie, IEEE J. Quantum Electron. QE-22, 1656 (1986).
[10]K. A. Harris, S. Hwang, D. K. Blanks, J. W. Cook, J. F. Schetzina, N. Otsuka, J. B. Baukus, and A. T. Hunter, Appl. Phys. Lett. 48, 396 (1986).
[11]S. Doniach and M. Šunjić, J. Phys. C 3, 285 (1970).
[12]C. Hsu, T. M. Duc, and J. P. Faurie (unpublished).
[13]T. Miller, A. P. Shapiro, and T. C. Chiang, Phys. Rev. B 31, 7915 (1985).
[14]R. Sporken, P. A. Thiry, E. Petit, J. J. Pireaux, R. Caudano, J. Ghijsen, R. L. Johnson, and L. Ley, Phys. Rev. B 35, 7927 (1987).
[15]G. K. Wertheim, S. B. DiCenzo, and D. N. E. Buchanan, Phys. Rev. B 33, 5384 (1986).
[16]S. Svensson, N. Martensson, E. Basilier, P. A. Mamquist, U. Gelius, and K. Siegbahn, J. Electron Spectrosc. Relat. Phenom. 9, 51 (1976).

[17]L. Ley, S. P. Kowalczyk, F. R. McFeely, and D. A. Shirley, Phys. Rev. B 10, 4881 (1974).
[18]V. L. Moruzzi, A. R. Williams, and J. F. Janak, Phys. Rev. B 10, 4856 (1974).
[19]W. Eberhardt, S. C. Wu, R. Garrett, D. Sondericker, and F. Jona, Phys. Rev. B 31, 8285 (1985).
[20]J. P. Faurie, A. Million, R. Roch, and J. L. Tissot, J. Vac. Sci. Technol. A 1, 1593 (1983); S. Sivananthan, X. Chu, J. Reno, and J. P. Faurie, J. Appl. Phys. 60, 1359 (1986).

062804JVA = 062804JVA

Pg. No.

Running Title: MCT junctions grown *in situ* by MBE

Mercury cadmium telluride junctions grown *in situ* by molecular-beam epitaxy

M. Boukerche, S. Yoo, I. K. Sou, M. De Souza, and J. P. Faurie
Department of Physics, University of Illinois at Chicago, Chicago, IL 60680

(Received 10 November 1988; accepted 17 February 1988)

The characterization of *n*-isotype mercury cadmium telluride heterojunctions made *in situ* by molecular-beam epitaxy is reported first. The cadmium composition of each side is 0.3 for the top material and 0.21 for the bottom. Both sides were doped with indium. Strong rectification with an ideality factor varying from 1.8 to 2.5 is shown. The forward bias occurs when the wide-band-gap material is biased negatively. The preliminary results of the first homojunctions made by the same technique are then presented. The cadmium composition was 0.27. The bottom *p*-type material was doped by stoichiometric deviation, whereas the top *n*-type material was doped with silicon. The device is sensitive to infrared radiation and it is found that the doping concentration is not uniform. We suggest that generation-recombination is limiting the device operation at high temperatures.

← INDENT

I. INTRODUCTION

In recent years, the mercury cadmium telluride (MCT) alloy has been recognized as the most important material formidinfrared applications. Its tunable band gap is also considered for near-infrared detection. Modern technologies to manufacture high-density array detectors require large high-quality epitaxial materials. The growth technique most commonly used industrially today is liquid phase epitaxy. Molecular-beam epitaxy (MBE) is one possible alternative since it has been shown that MBE is able to produce high-quality material.[1] Furthermore, excellent uniformities in composition and thickness along with uniform properties have been obtained for MCT epitaxial layers on 2-in.-diam GaAs substrates.[2] The key issue now is to qualify the MBE material through device characterization. The demonstration of *in situ* doping and junction formation, without annealing treatments, is a very important contribution towards this goal. We reported last year unexpected barrier formation in the first *n*-isotype abrupt heterojunctions.[3] We will show here that such effects can be avoided. Strong rectification is then observed. We will also present the first results on homojunctions doped *in situ* with silicon.

II. HETEROJUNCTIONS

N-isotype abrupt heterojunctions were grown on CdTe(111)/GaAs(100) combination substrates as previously reported. The CdTe buffer layer was 2.2 μm thick. The narrow band-gap layer was then grown with a cadmium composition $X = 0.21$ and a donor concentration of 4×10^{15} cm^{-3}, as determined by Hall measurements. When the MCT material thickness reached 3 μm, the Cd content was abruptly increased to 0.30. This final layer was then grown with a thickness of 0.5 μm. Its donor concentration is not precisely known but is estimated to be in the low 10^{15} cm^{-3} range from the growth conditions. Both sides of the junction were doped with indium as previously reported.[4] The other effusion cells used contained Te, CdTe, and Hg, respectively. The substrate temperature was maintained at 190 °C and the growth rate was 5–7 Å/s. To avoid the composition burst observed previously at the heterojunction interface,[3] the distance between the cells and their shutters was increased. Mesa devices were then made with In contacts and ZnS passivation. The top contact area was 10^{-4} cm^2. The processing temperature never exceeded 60 °C.

As seen in Fig. 1 strong rectification was observed. Forward conduction occurred for a positive bias applied to the narrow-band-gap material. The average R_0A of the 30 devices measured reached 10^3 $\Omega \times cm^2$ at liquid-nitrogen temperature. A value of 10^4 $\Omega \times cm^2$ was observed on one device. We conclude that the device operation is limited by the wide-band-gap material where most of the depletion occurs. The I/V curves were least-squares fitted at each temperature to the usual following diode equation. Series resistance had to be included since it is unavoidable in such thin devices and low doping levels.

$$I = I_s\{\exp[q(V - R_sI)/nkT] - 1\}, \quad (1)$$

where I_s is the saturation current, R_s the series resistance, n the ideality factor, I the current density, V the bias, k the Boltzman constant, q the electronic charge, and T the absolute temperature.

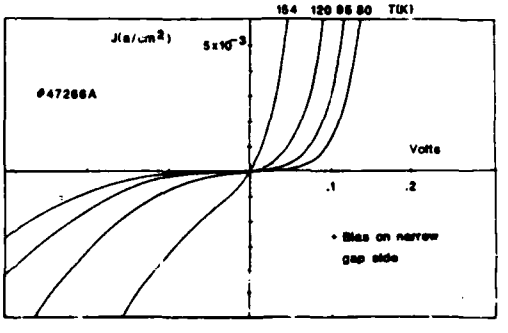

FIG. 1. Current vs voltage curves of the heterojuncton device.

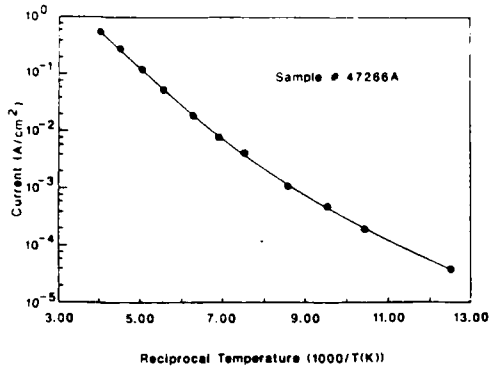

FIG. 2. Variation of the current prefactor I_t in Eq. (1) with the reciprocal temperature.

The quality of the fitting was excellent at all the temperatures with four decades of forward current variation. Its reliability above 200 K was questionable since the curves were basically Ohmic. The ideality factor n varied from 1.8 at 200 K to 2.5 at low temperatures. The activation energy of I_t was consistently close to 125 meV at high temperatures, whereas at low temperatures it decreased to around 80 meV depending on the device tested (Fig. 2). Capacitance measurements are believed to be unreliable since series resistance could not be neglected and the top material thickness was very thin. A calculation of the expected band profile of the heterojunction is shown in Fig. 3. The method used has been previously described.[3] We assumed a valence-band offset equal to 10% of the band-gap difference between the two sides at 80 K, and doping levels of 4×10^{15} cm^{-3} and 2×10^{15} cm^{-3} in the narrow- and wide-band-gap sides, respectively. (If the valence-band offset would be taken as 20% of the band gap, the phenomenologic discussion which follows would not be changed.) This calculation gives a depletion layer thickness more than 0.3 μm in the wide-band-gap material. This is very close to the top contact position. The barrier height between the top of the spike and the Fermi level is 104 meV. The spectral response of one device reverse biased at 50 mV is shown in Fig. 4. A maximum is seen at 8-μm wavelength. It can be noticed that the photosignal does not seem to follow the usual internal photoemission theory on the cutoff side of the curve. The photoresponse signal displays a tendency towards a more linear relationship with the photon energy. This could be due in part to a photoconductive contribution of the series resistance around the mesa. The narrow-band-gap side near the heterojunction is believed to be heavily degenerate at 80 K, in strong accumulation (see Fig. 3). The energy distribution range of the photoemitted electrons is then limited to a few kT. This situation can lead to a linear relationship between the photon energy and the photosignal.[5] A linear extrapolation of the experimental curve in the cutoff region would then give a barrier height ϕ_B equal to 130 meV. The devices looks like a metal–semiconductor Schottky diode[6] where the metal would be the degenerate narrow-band-gap material. However, the equivalent barrier height, i.e., the energy difference between the top of the spike and the Fermi level, is a function of the bias. Anderson[6] showed that an ideality factor >1 is expected, and that the reverse current should not saturate. The builtin potential is 26 meV on the narrow band gap and 93 meV on the other side. At low forward bias the ideality factor should be close to 1.28. The fact that n equals or exceeds 2 makes us conclude that thermionic emission is not the only transport involved, even at high temperatures. This is also supported by the following argument. The variation versus temperature of I_t deduced from the fitting to Eq. (1) closely matches the variation of the current measured at low forward bias. According to the Anderson[6] model, at fixed low voltages, the current should vary as $T^{1/2}\exp(-qV_D/kT)$, where T is the absolute temperature and V_D is the electrostatic potential drop across the wide-band-gap material side. The calculation shows that V_D, at zero bias, should decrease when the temperature increases. For example, it should be approximately equal to 40 meV at 250 K. This is in contradiction with the measurements since the activation energy of $I/T^{1/2}$

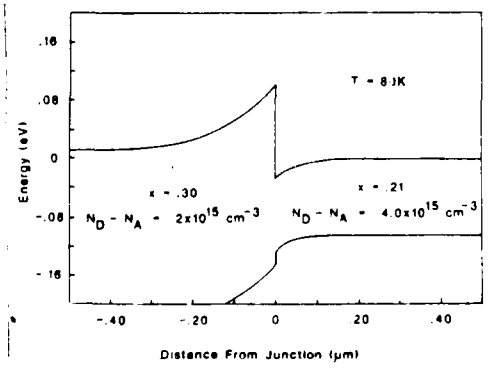

FIG. 3. Energy band profile calculated for the heterojunction. Two-dimensional quantization has been neglected. The energy reference is the Fermi level.

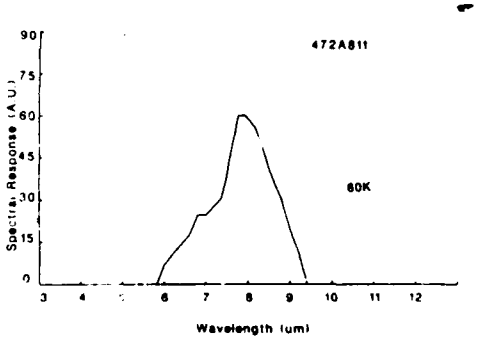

FIG. 4. Spectral response of the heterojunction at 80 K.

is equal to 120 meV at high temperatures.

We suggest that generation–recombination mechanisms in the $x = 0.3$ material play an important role at high temperatures. Tunneling effects are expected at low temperatures in such narrow-band-gap materials, they are certainly responsible for the increase of n to 2.5 at 80 K. However, the slope of log I/V still increases down to this temperature, and another transport process is still present. If thermionic emission is the main relevant mechanism in the intermediate temperature range, the activation energy of I_s (82 meV) would be in reasonable agreement with the calculated value of V_{D2} (93 meV).

III. HOMOJUNCTIONS

The epitaxial layer was grown on CdTe(111)/GaAs(100) substrate at the same temperature as before (190 °C). The stoichiometric conditions were adjusted to produce p-type material with a thickness of 4.2 μm. The silicon n-type doping flux was then added on the crystal during the remaining 1 μm material grown subsequently by opening the corresponding shutter. The other growth conditions were identical to the ones reported above. Hall measurement of the layer as grown gave an n-type doping level of 5×10^{16} cm^{-3} in the top material neglecting the contribution of the p-type material. This was relevant since this measurement showed an n-type fully ionized behavior below 250 K (flat curve). After etching of the n-type material, the same technique showed that the remaining material was p type with a level of 2×10^{16} cm^{-3}. Freeze out was present down to the lowest temperature measured (28 K). The cadmium composition was determined at room temperature by Fourier transform infrared (FTIR) transmission measurements. The value calculated for an absorption coefficient of 1000 cm^{-1} was $x = 0.27$. Mesa devices were subsequently processed at low temperature (below 65 °C). The n-type materials were contacted with indium and gold, respectively. The area of the devices was 1.5×10^{-4} cm^2. The I/V curves in Fig. 5 were measured with a cryogenic probe station. They show good rectification, forward bias occurring when the top n-type material is biased negatively as expected. We can see in Fig. 6 that illumination by a blackbody at 600 K generates a reverse photocurrent. The variation of R_0A versus temperature in Fig. 7 follows a constant slope at high temperatures, and progressively saturates down to 90 K, decreasing slightly thereafter. At liquid-nitrogen temperature, the device is expected to be limited by tunneling and edge leakage since no passivation was used and the structure is not gated. Also, the field of view of the room temperature background was 180°, so the value of R_0A is not entirely limited by the junction material. Since the n-type material is degenerate at 80 K, most of the depletion layer should be on the p side. At zero bias the capacitance is 30% smaller than expected from the doping levels. It decreases with reverse bias but $1/C^2$ does not follow a straight line. We conclude that the doping is not uniform, and that the silicon probably diffused in the p side. The I/V data were fitted to Eq. (1). The ideality factor varied from 2.1 at high temperature to 3.0 at 80 K. Since the same time R_0A varies nearly as $1/n_i$, where n_i is the intrinsic carrier concentration, we suggest that generation–recombination currents in the depletion region could be dominant above 160 K.[7] Further analysis of these devices will be published elsewhere.[8]

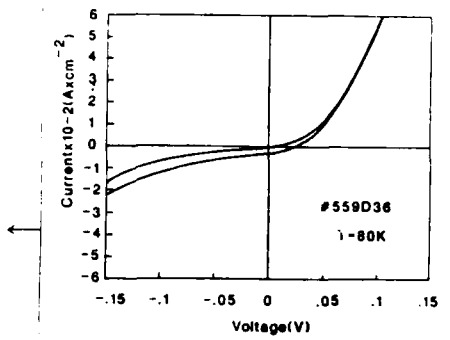

FIG. 6. I/V curve of the homojunction at 80 K, with and without illumination from a blackbody at 600 K. The room-temperature background field of view is 180°.

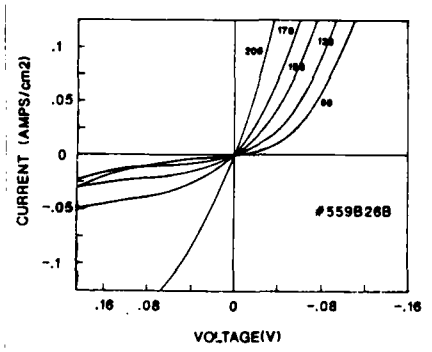

FIG. 5. Current vs voltage curves for the homojunction device.

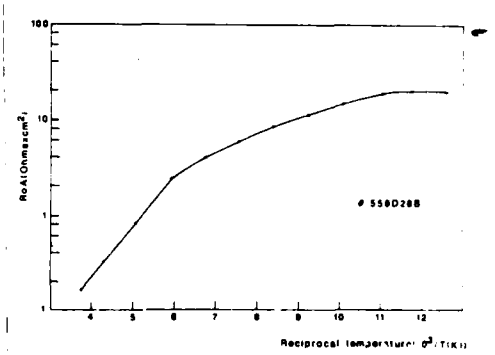

FIG. 7. Variation of the zero bias resistance of the homojunction vs reciprocal temperature. Background field of view is 180°.

IV. CONCLUSION

The first rectifying MCT devices made *in situ* by MBE have been described. The previous composition burst during heterojunction formation could be eliminated by proper growth condition. The strong rectification measured shows that the conduction-band discontinuity is abrupt, and that the interface state density between the two materials is negligible.

The homojunction presented also showed strong rectification and generated a photovoltaic current upon infrared illumination.

These preliminary results are intended to represent a first step in the understanding of *in situ* junction formation using the MBE technique. All the native defects are still present in the material since it is not annealed under mercury pressure, as is commonly the case for *ex situ* made junctions. The control of doping is also a very difficult task to achieve in this II–VI ternary alloy. In addition all the measurements were made with 180° field of view and a probe station where some residual strain is unavoidable during probing.

Further material characterizations and device modeling are then needed to confirm the generation–recombination process suggested and also why the diffusion limited regime is not observed in the homojunction at high temperature.

ACKNOWLEDGMENTS

The technical help of Z. Ali and S. Farook was greatly appreciated. This work was funded by DARPA under Contract No. F49620-87-C-0021. One of us (MDS) is also supported by a scholarship from C. N. Pq, Brazil.

[1] S. Sivananthan, M. D. Lange, X. Chu, and J. P. Faurie, J. Vac. Sci. Technol. A, March-April (1988).
[2] M. D. Lange, S. Sivananthan, X. Chu, and J. P. Faurie, Appl. Phys. Lett. Appl. Phys. Lett. 52, 978 (1988).
[3] M. Boukerche, I. K. Sou, M. De Souza, S. Yoo, and J. P. Faurie, J. Vac.Sci. Technol. A 5, 3119 (1987).
[4] M. Boukerche, J. Reno, I. K. Sou, C. Hsu, and J. P. Faurie, Appl. Phys. Lett. 48, 1733 (1986).
[5] R. Williams, *Semiconductors and Semimetals* (Academic, New York, 1970), Vol. 6.
[6] R. L. Anderson, Solid State Electron. 5, 341 (1962).
[7] M. B. Reine, A. K. Sood, and T. J. Tredwell, *Semiconductors and Semimetals* (Academic, New York, 1981), Vol. 18.
[8] M. Boukerche, S. Yoo, I. K. Sou, M. D. Souza, and J. P. Faurie (unpublished results).

END

DATE
FILMED

9-88